Binghamton University
The Open Repository @ Binghamton (The ORB)

Undergraduate Honors Theses | Dissertations, Theses and Capstones

Spring 5-11-2022

Synthesis and characterization of hydrazine derivatives of coumarin for bioorthogonal chemistry inside cells

Akiva J. Grimaldi
Binghamton University--SUNY, agrimal2@binghamton.edu

Follow this and additional works at: https://orb.binghamton.edu/undergrad_honors_theses

 Part of the Chemistry Commons

Recommended Citation

Grimaldi, Akiva J., "Synthesis and characterization of hydrazine derivatives of coumarin for bioorthogonal chemistry inside cells" (2022). *Undergraduate Honors Theses*. 19.
https://orb.binghamton.edu/undergrad_honors_theses/19

This Thesis is brought to you for free and open access by the Dissertations, Theses and Capstones at The Open Repository @ Binghamton (The ORB). It has been accepted for inclusion in Undergraduate Honors Theses by an authorized administrator of The Open Repository @ Binghamton (The ORB). For more information, please contact ORB@binghamton.edu.

SYNTHESIS AND CHARACTERIZATION OF HYDRAZINE DERIVATIVES OF COUMARIN FOR BIOORTHOGONAL CHEMISTRY INSIDE CELLS

BY

AKIVA J. GRIMALDI

THESIS

Submitted in partial fulfillment of the requirement for

Distinguished Independent Work in Chemistry

in Harpur College of Arts and Sciences of

Binghamton University

State University of New York

2022

© Copyright by Akiva Joseph Grimaldi 2022

All Rights Reserved

Accepted in partial fulfillment of the requirement for

Distinguished Independent Work in Chemistry

in Harpur College of Arts and Sciences of

Binghamton University

State University of New York

2022

May 11, 2022

Susan L. Bane, Faculty Advisor

Department of Chemistry, Binghamton University

Rebecca Kissling, Member

Department of Chemistry, Binghamton University

Alistair Lees, Member

Department of Chemistry, Binghamton University

Table of Contents

List of Figures

List of Tables

List of Schemes

Synthesized Molecules

Abstract

Protein carbonylation is one manifestation of oxidative stress, which is characteristic of many diseases. Our lab has developed several coumarin-hydrazine based fluorescent probes capable of detecting carbonylation in live cells via the formation of hydrazone conjugates. As an effort to expand and improve on these achievements, this work presents new data regarding the synthesis and characterization of three such probes. Two of the probes—julolidine coumarin hydrazide (JCH) and trifluoromethyl coumarin hydrazine (TFCH)—were previously synthesized by our lab. Here, JCH is studied in terms of its reaction speed and fluorescence enhancement in acylhydrazone formation with aldehydes under various conditions and catalytic schemes. For TFCH, the previously developed synthetic scheme is replicated, and the molecule is subjected to analysis of its reaction with various aldehydes, as well as stability studies. The synthesis of a third probe—coumarin acid hydrazine (CAH)—is developed, adding a novel analog to our library. CAH is substituted with a carboxylic acid at the 4-position, which may confer the benefit of enhanced water solubility and situates it as the precursor to an ester substituted derivative for future work.

Acknowledgements

A great number of people have guided and inspired me throughout my time at Binghamton University. While there are far too many to mention everyone here, I would like to recognize those who were most influential to this work:

- Dr. Bane, for serving as my mentor and advisor, always being there to discuss my work (or anything aside from it), and providing this opportunity by taking me into the lab and giving me the freedom to grow.
- Madeleine Beaulieu, for teaching me most of the hands-on skills I used for synthesis, your patience to talk through every little difficulty I've encountered, and for being the person to ask whenever anyone has a question in lab.
- Olivia Morini, for joining me this semester and lending a very useful helping hand, for our conversations in lab, and for giving me an opportunity to pass on what I've learned.
- Everyone in the Bane Lab, for always being a pleasure to interact and work with.
- Juergen Schulte, for indispensable assistance with NMR spectroscopy.
- Dr. Saptarshi Ghosh, for getting me started in the lab and for the samples of JCH.
- Dr. Anthony Sorrentino, for synthesizing TFCH and for information in his honors thesis.
- Dr. Kissling, for helping inspire my enthusiasm for organic chemistry and for serving on this committee.
- Dr. Lees, for a fantastic class in photochemistry and for serving on this committee.
- The Binghamton University Department of Chemistry, for helping to organize all I've done within chemistry research and the major.
- My friends, for more than I can possibly express.
- My family, for everything.

Introduction

Background

Oxidative stress is characteristic of many diseases, and involves the production of reactive oxygen species (ROS) including radicals and peroxides. These species cause cellular damage via the oxidation of biomolecules.[1] Protein carbonylation is one such type of oxidative damage, and affected proteins may exhibit improper folding and/or loss of function.[2] Furthermore, carbonylated proteins can form aggregates that inhibit proteasome activity and thus prevent their own degradation.[2]

Various methods have been employed in the identification and quantification of protein carbonylation. Among the most frequently used chemical methods is bioorthogonal hydrazone or oxime formation, using probes that can then be analyzed through immunofluorescent imaging, spectrophotometry, fluorescence, or other techniques.[3] These methods have traditionally been applied to non-living systems, such as fixed cells or extracts, hindering the scope of their utility.

In 2015, our lab demonstrated the observation of intracellular carbonyls in live cells using a hydrazine derivative of coumarin—named coumarin hydrazine (CH)—which reacts with carbonyls to form hydrazone conjugates (Figure 1).[4] However, the conjugates of CH are not very photostable, and require high energy light for excitation (~360 nm), which can damage live cells and tissue.[4] Since then, work has focused on developing coumarin hydrazine-based probes with improved properties. In addition to higher photochemical stability and a redder absorbance, ideal properties include a high extinction coefficient, a large Stokes shift—which decreases overlap between the light emitted by the probe and its own range of absorbance, a higher quantum yield of the hydrazone conjugate—which leads to an enhanced fluorescent signal upon reaction of the

probe with carbonyls, and good solubility under biological conditions. Trifluoromethylcoumarin hydrazine (TFCH), another probe more recently developed by our lab, exhibits many of these desirable properties and has successfully been used to detect carbonylation due to oxidative stress in live cells and in renal cells treated with nephrotoxic drugs.[5]

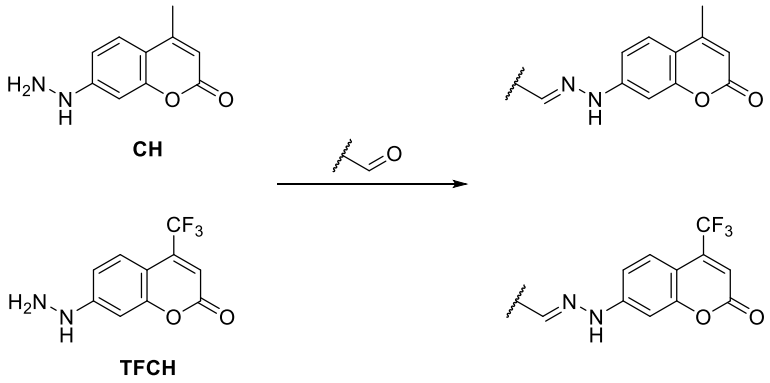

Figure 1. CH, TFCH, and their general reaction with aldehydes to form hydrazone conjugates.

Objectives

Building on this previous work, the properties of two probes previously synthesized in our lab are examined. The reaction speed and fluorescence enhancement of acylhydrazone formation of julolidine coumarin hydrazide (JCH) with salicylaldehyde are qualitatively studied in organic solvent without catalysis and under conditions of acid and nucleophilic catalysis. The analogous reaction with propanal in phosphate buffer is also assessed, as these conditions better simulate the aliphatic carbonyls produced by oxidative stress in biological systems. TFCH is synthesized according to its previously developed synthetic scheme. Hydrazone formation of

TFCH with propanal, 3-formyl-tyrosine, and salicylaldehyde in phosphate buffer are compared, with attention given to reaction speed and solubility of the conjugate. Finally, the long-term stability of TFCH is investigated by observation of elevated fluorescence in a DMSO stock solution stored at room temperature for over a year, which is suggestive of highly fluorescent degradation products. For a freshly prepared DMSO stock, 20 freeze-thaw cycles are shown to cause no difference in the fluorescence of TFCH, nor in its reaction with propanal.

Additionally, this work develops the synthesis of a novel coumarin hydrazine-based probe substituted with a carboxylic acid at the 4-position. This substitution was selected because a carboxylic acid will likely give the molecule enhanced aqueous solubility compared to similar coumarin fluorophores. The 4-position was chosen because of the observed trend of larger Stokes shifts among 7-aminocoumarins substituted with electron withdrawing groups at the 4-position, relative to their 3-substituted analogs.[6] Moreover, the carboxylic acid could serve the precursor for an ester substitution, which would be of particular interest because drugs and other molecules of interest could be linked at this position. One such potential application is the creation of a proteolysis targeting chimera (PROTAC). PROTACs are composed of a protein-binding ligand linked to a E3 ligase recruiting element (E3RE), which triggers ubiquitination and degradation of the target protein.[7] Here, the hydrazine would serve as the protein-binding ligand, targeting carbonylated proteins, and an E3RE, such as a thalidomide derivative, would be linked at the ester. This may offer an advantage over other PROTACs in that it would allow fluorescence visualization of the location and extent of carbonylation, in addition to executing its usual role in facilitating degradation of the damaged proteins.

Results

Julolidine Coumarin Hydrazide

Synthesis

Julolidine coumarin hydrazide (JCH; Figure 2) was conceptualized and synthesized in our lab by Dr. Ghosh. NMR analysis of the synthesized and purified samples showed that each contained between 0.5 and 4 percent of the ethyl ester precursor to JCH. This intermediate is highly fluorescent and would significantly interfere with the observed photochemical properties of JCH, and especially its fluorescence enhancement upon acylhydrazone formation. A small sample of JCH had been cleansed of the ester by Dr. Ghosh via reversed phase high performance liquid chromatography, and this sample was used for all experiments reported herein.

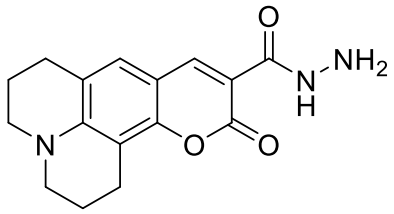

Figure 2. Structure of JCH

Kinetic and Spectroscopic Studies

The kinetics of acylhydrazone formation from JCH and salicylaldehyde (Figure 3) were examined under various reaction conditions. In each case, 10 μM of JCH was reacted with 100 μM of salicylaldehyde, yielding pseudo first-order kinetics plots. The fluorescence emission spectra of the products were compared to those of JCH prior to reaction.

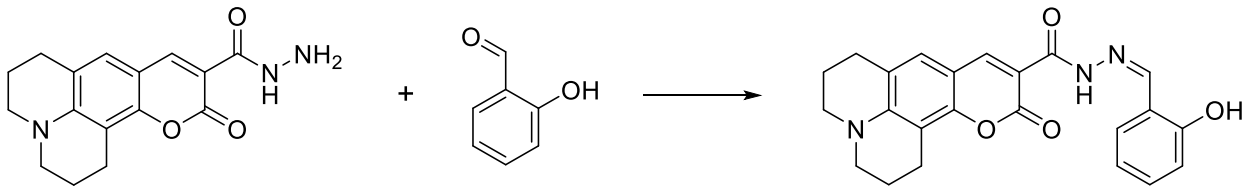

Figure 3. Reaction of JCH and salicylaldehyde to form an acylhydrazone conjugate.

First, the uncatalyzed reaction was assessed in ethanol, methanol, and DMSO. The kinetics plots (Figure 4) demonstrate that the reaction was not complete after three hours in any of the solvents. Moreover, the reaction hardly proceeded in DMSO, likely because the reaction mechanism requires a proton source.

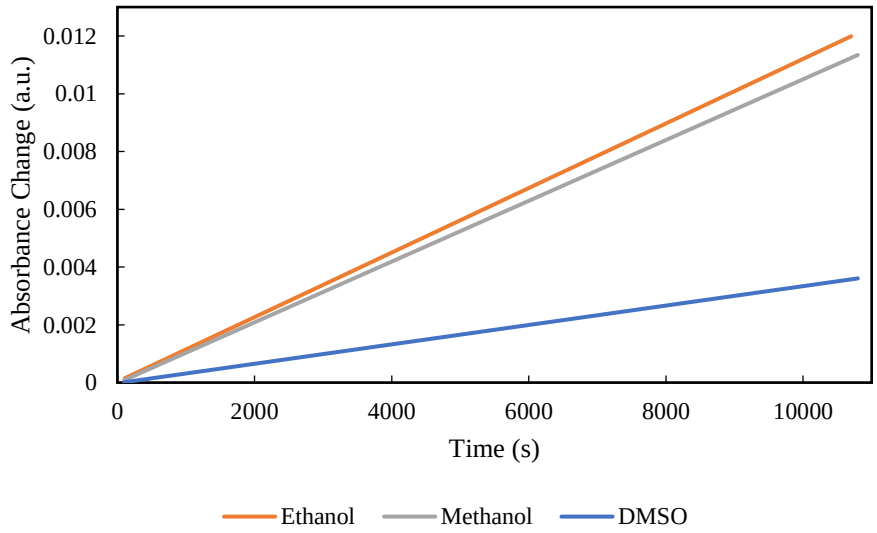

Figure 4. Reaction kinetics of acylhydrazone formation from JCH (10 µM) and salicylaldehyde (100 µM) in ethanol, methanol, and DMSO. Tracked by absorbance change at 450 nm.

The fluorescence emission spectra from before and after the reactions in methanol and ethanol are shown in Figure 5. Emission intensities (here and throughout this work, unless otherwise noted) were corrected by absorbance at the excitation wavelength, so emission intensities are reflective of the relative quantum yields. These results demonstrate good fluorescence enhancement even before reaction completion. The enhancement was stronger in ethanol than in methanol, and gave an over four-fold increase in emission intensity.

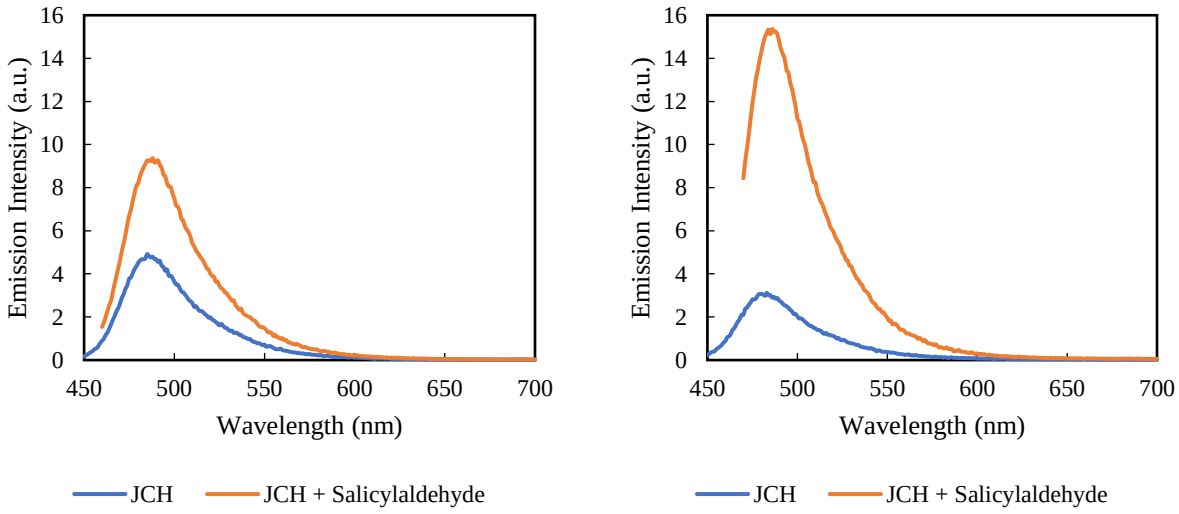

Figure 5. Emission spectra of JCH and the reaction products of JCH and salicylaldehyde in methanol (left) and ethanol (right). JCH and products were excited at 438 and 450 nm, respectively.

Inspired by its need for a proton source, the reaction was next tested in the presence of 0.25 percent acetic acid, which served as an acid catalyst. Again, this was completed in ethanol, methanol, and DMSO. The kinetics plots (Figure 6) show good rate enhancement for the reactions in ethanol and methanol, which were not complete at three hours but were nearing a plateau. Only slight enhancement was observed in DMSO.

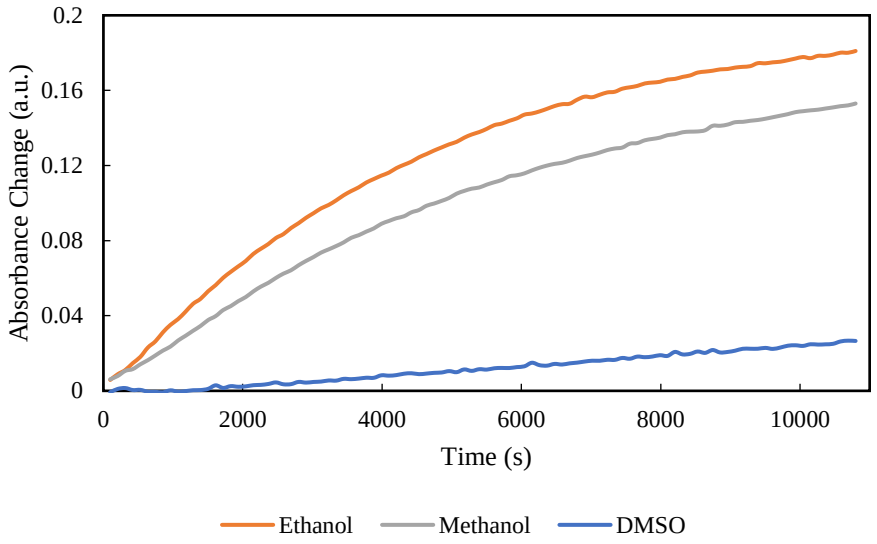

Figure 6. Reaction kinetics of acylhydrazone formation from JCH (10 µM) and salicylaldehyde (100 µM) in ethanol, methanol, and DMSO, in the presence of 0.25% acetic acid catalyst. Tracked by absorbance change at 460 nm.

The emission spectra from before and after the reactions in ethanol and methanol (Figure 7) show a dramatic loss of fluorescence enhancement compared to the uncatalyzed reaction. Evidently, an acidic environment leads to a strong increase in JCH fluorescence, without having a parallel effect on the fluorescence of the acylhydrazone.

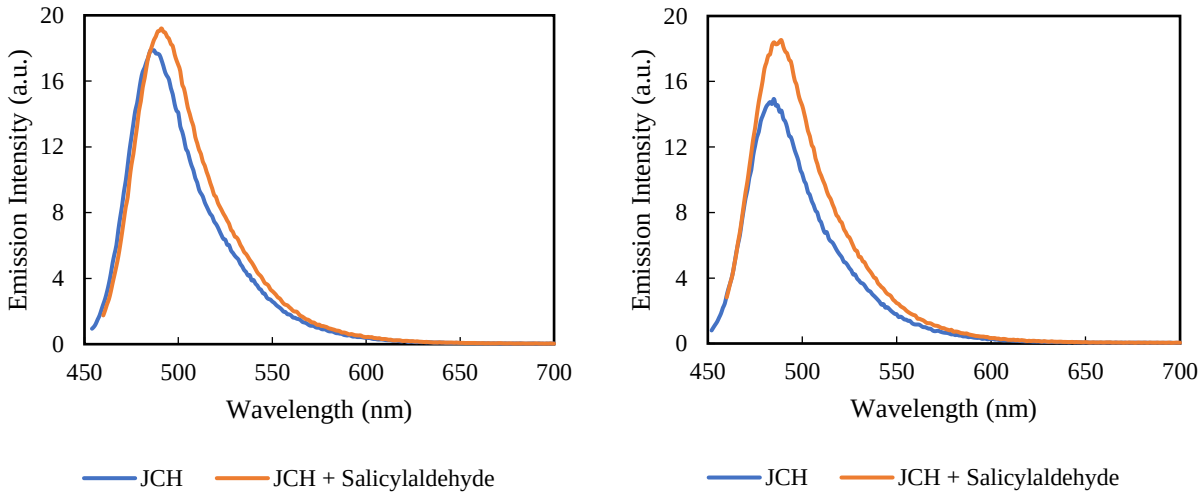

Figure 7. Emission spectra of JCH and the reaction products of JCH and salicylaldehyde in methanol (left) and ethanol (right), in the presence of 0.25% acetic acid catalyst. JCH and products were excited at 444 and 450 nm, respectively.

In an attempt to obtain reaction completion in a more reasonable length of time, the concentration of acetic acid was increased to 1 percent in ethanol. The kinetics plots and emission spectra from before and after the reaction are presented together in Figure 8. The reaction demonstrated satisfactory rate enhancement and completion within three hours. Moreover, while still lower than that of the uncatalyzed reaction, fluorescence enhancement was much improved compared to the reaction catalyzed by 0.25 percent acetic acid. A likely explanation is that for the 10 μM concentration used, the maximum effect of acid on JCH fluorescence had already been reached at 0.25 percent acetic acid, but fluorescence of the product increased because more acylhydrazone was formed in three hours with 1 percent acetic acid.

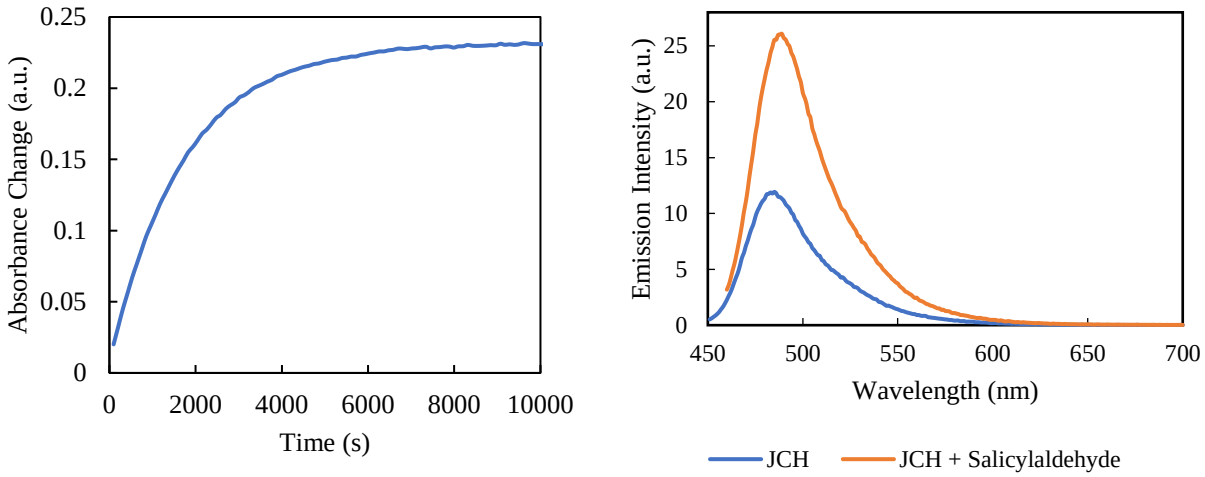

Figure 8. Left: Reaction kinetics, tracked by absorbance change at 460 nm, of acylhydrazone formation from JCH (10 µM) and salicylaldehyde (100 µM) in ethanol containing 1% acetic acid catalyst. Right: Fluorescence emission spectra from before (λ_{ex} = 441 nm) and after (λ_{ex} = 450 nm) this reaction.

To address the slow rate of acylhydrazone formation while avoiding the use of acidic conditions, the effect of nucleophilic catalysis was studied using aniline. As shown in Figure 9, 200 µM salicylaldehyde was first reacted with aniline to form a more reactive imine intermediate, which was then reacted with 10 µM JCH to yield the acylhydrazone conjugate. In making the reaction solutions, the solution in which the imine was formed was diluted by a factor of two (while the aniline concentration was kept constant). Hence, these reactions can be compared to the reaction of 100 µM salicylaldehyde and 10 µM JCH under other conditions.

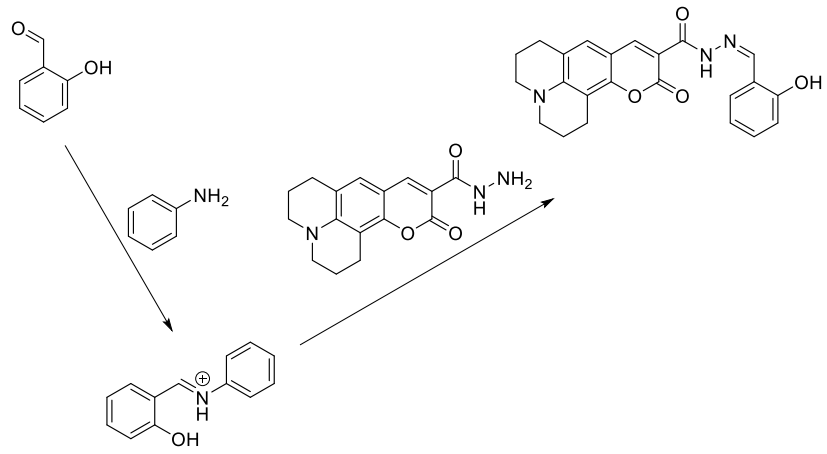

Figure 9. Nucleophilic catalysis involving imine formation using aniline, followed by reaction with JCH.

Using methanol as the solvent, 200 µM salicylaldehyde was reacted with 1, 10, and 100 mM aniline, and the resulting solutions were reacted with 10 µM JCH. Both sets of reactions were tracked by absorbance change, and the kinetics plots are presented in Figure 10. Satisfactory conversion to the imine was obtained with both 10 and 100 mM concentrations of aniline, although the reaction was complete within three hours only when 100 mM was used. The reaction of JCH with the aniline-salicylaldehyde imine was moderately faster with 100 mM aniline, and neither reaction was complete at five hours.

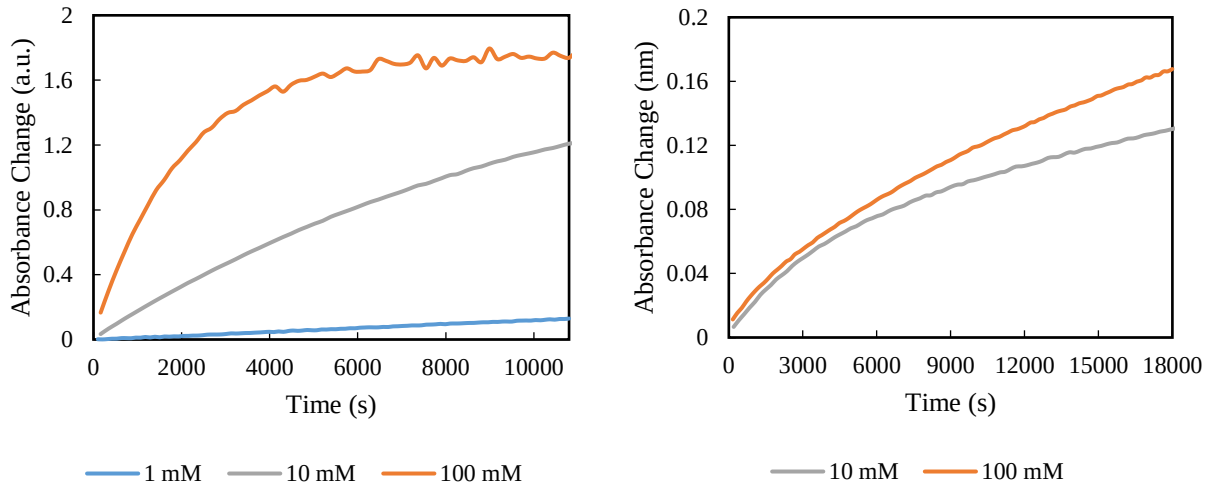

Figure 10. Left: Reaction kinetics, tracked at 340 nm, of imine formation from 200 µM salicylaldehyde and varying concentrations of aniline in methanol. Right: Reaction kinetics, tracked at 462 nm, of acylhydrazone formation from the resulting salicylaldehyde-aniline imine solutions, diluted by a factor of two, and 10 µM JCH in methanol.

Emission spectra (Figure 11) were collected before and after each reaction. The spectrum from after the reaction using 10 mM of the aniline catalyst shows approximately six-fold fluorescence enhancement compared to unreacted JCH. But despite the greater progress achieved by the reaction, the enhancement was almost completely diminished when 100 mM aniline was used. This observation was attributed to aggregation of the acylhydrazone product in the presence of high concentrations of aniline, which was indicated in the absorbance spectrum of the reaction products.

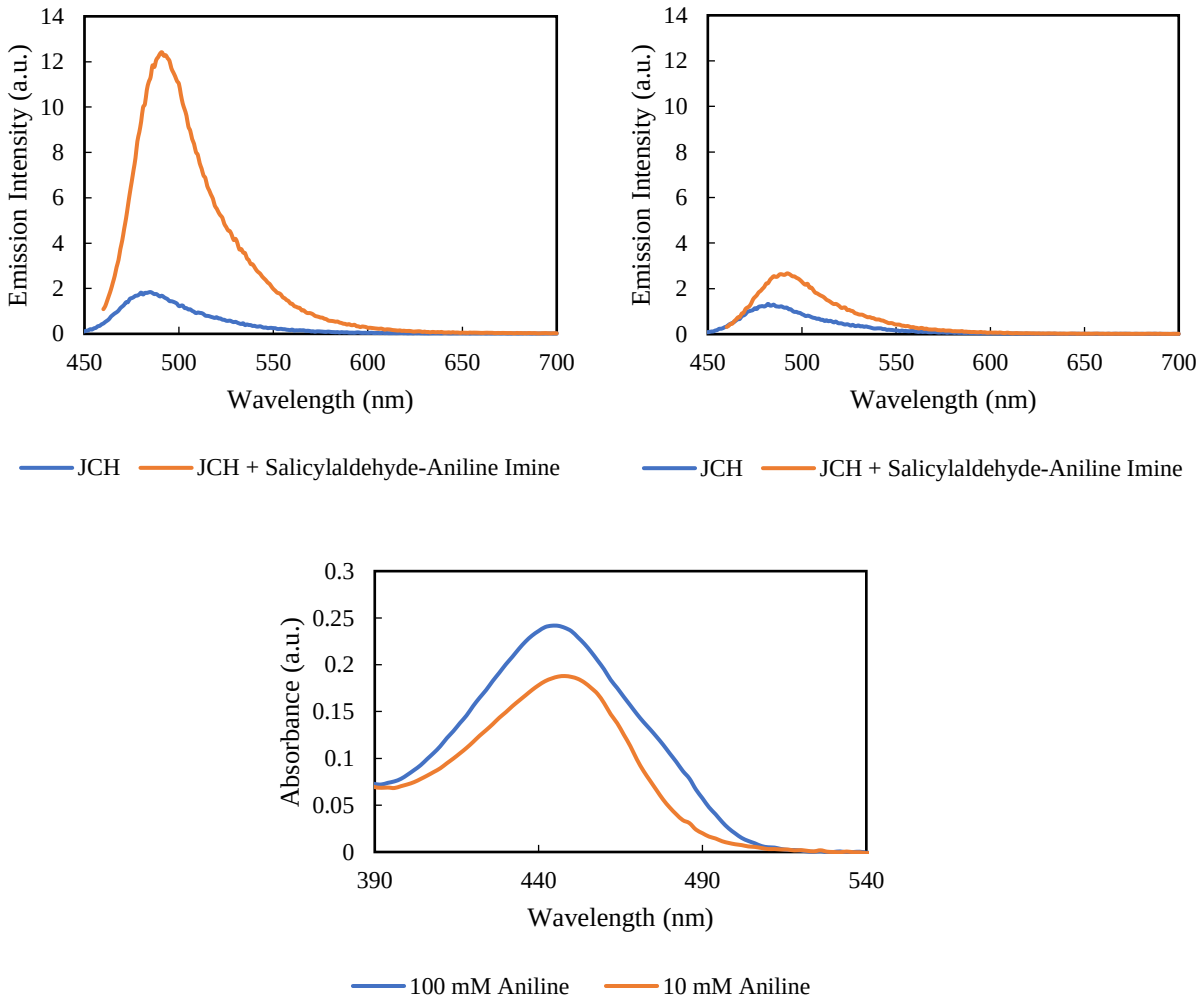

Figure 11. Emission spectra of JCH and the reaction products of JCH and the salicylaldehyde-aniline imine, in the presence of 10 mM (top left) and 100 mM (top right) concentrations of aniline, in methanol. Bottom: Absorbance spectra of the reaction products. Aggregation is seen as a broadening of the spectrum in 100 mM aniline.

The final experiment involving JCH was the reaction of 5 µM JCH and 5 µM propanal in 10 mM phosphate buffer (pH 7.4). This reaction (Figure 12) is analogous to the acylhydrazone formation of JCH with salicylaldehyde, except that here the aldehyde is aliphatic rather than aromatic. It was completed primarily for the purpose of comparison to the other coumarin-based probes examined in this work, which were reacted with propanal in phosphate buffer.

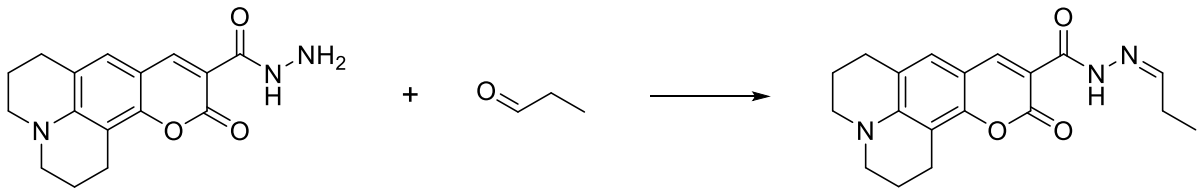

Figure 12. Acylhydrazone formation by reaction of JCH and propanal.

The reaction kinetics, as well as the absorbance and emission spectra of the products and JCH, are depicted in Figure 13. They show a relatively fast reaction (as compared to the salicylaldehyde reactions) but only moderate fluorescence enhancement. Although the conditions were not acidic, the high fluorescence of unreacted JCH resembles that observed under the conditions of acid catalysis in alcohol, suggesting the same causative mechanism in both cases.

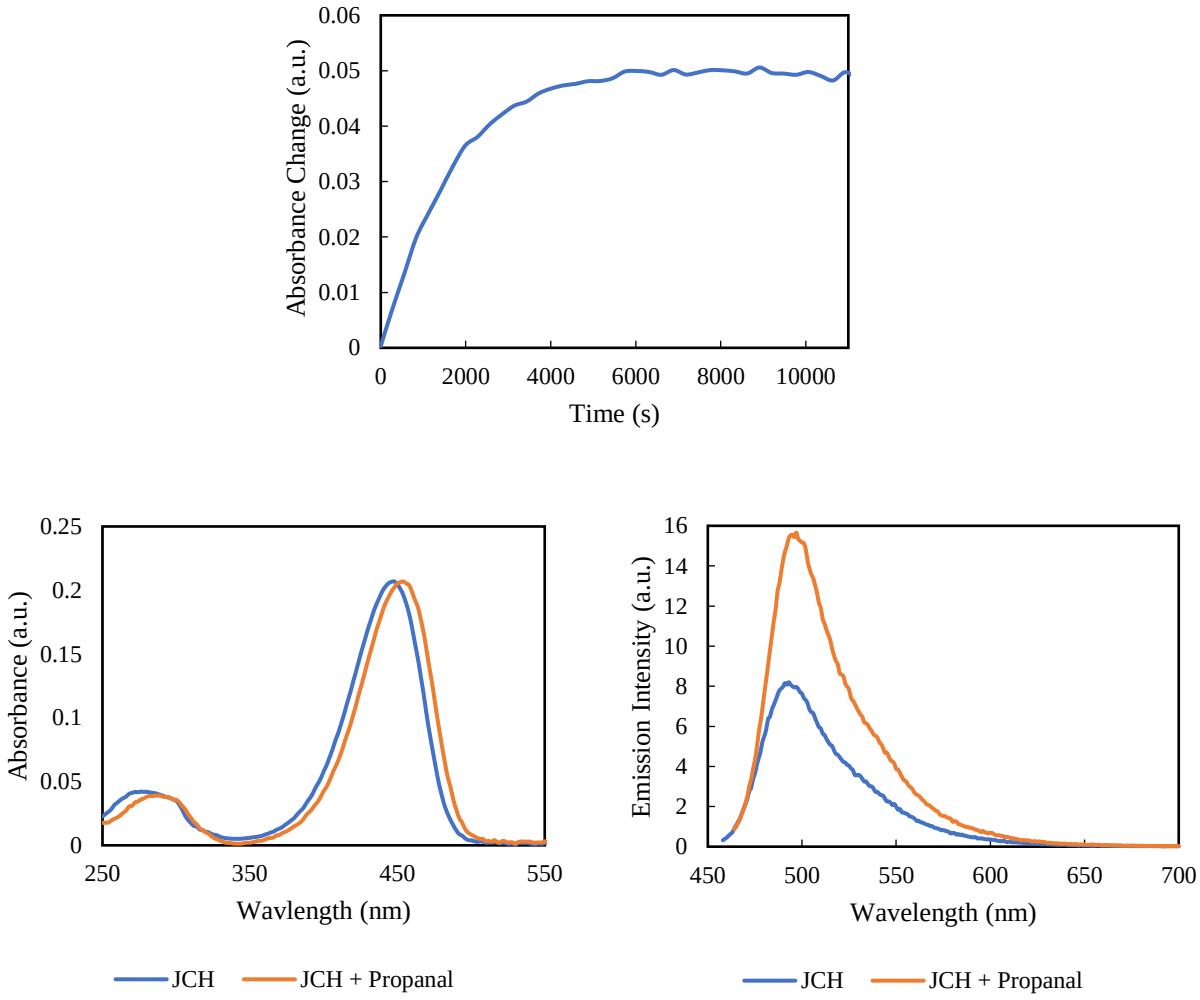

Figure 13. Top: Reaction kinetics, tracked by absorbance change at 472 nm, of acylhydrazone formation from JCH (5 µM) and propanal (500 µM) in 10 mM phosphate buffer (pH 7.4). Bottom left: Absorbance spectra from before and after this reaction. Bottom right: Fluorescence emission spectra before (λ_{ex} = 448 nm) and after (λ_{ex} = 454 nm) reaction.

Table 1 gives the absorbance and emission maxima for JCH and the acylhydrazone conjugate of JCH and salicylaldehyde or propanal in 10 mM aniline in methanol, 1 percent acetic acid in ethanol, and 10 mM phosphate buffer. These reactions were selected because they reached completion, and therefore, given the excess of aldehyde used, the photochemical

properties of their products are representative of the conjugate. Notably, under all solvent conditions, the absorbance and emission maxima are red-shifted in going from JCH to the acylhydrazone. The magnitude of the shift is greater for the absorbance than for the emission, leading to a slightly smaller Stokes shift for the conjugate compared to JCH, although it remains in the range of approximately 35-50 nm for both.

Table 1. Absorbance and emission maxima of JCH and the reaction products of JCH and salicylaldehyde or propanal, in varied reaction solvents.

Solvent	Molecule	Absorbance Maximum (nm)	Emission Maximum (nm)
10 mM aniline in methanol	JCH	436	485
	JCH + Salicylaldehyde	446	491
1% acetic acid in ethanol	JCH	442	485
	JCH + Salicylaldehyde	450	488
10 mM phosphate buffer (pH 7.4)	JCH	446	493
	JCH + Propanal	452	497

Trifluoromethyl Coumarin Hydrazine

Synthesis

Trifluoromethyl coumarin hydrazine (TFCH; Figure 14) was first synthesized by Dr. Anthony Sorrentino. The synthetic scheme was published in his undergraduate honors thesis[8] and was replicated, with minor modifications, to prepare TFCH for use in the experiments presented here.

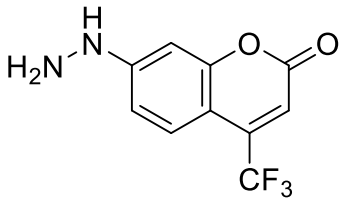

Figure 14. Structure of TFCH

Scheme 1 illustrates the synthetic path taken to obtain the molecule. Samples of TFCH previously synthesized in our lab were also used in some of the experiments. The identity and purity of all samples were confirmed by NMR prior to use.

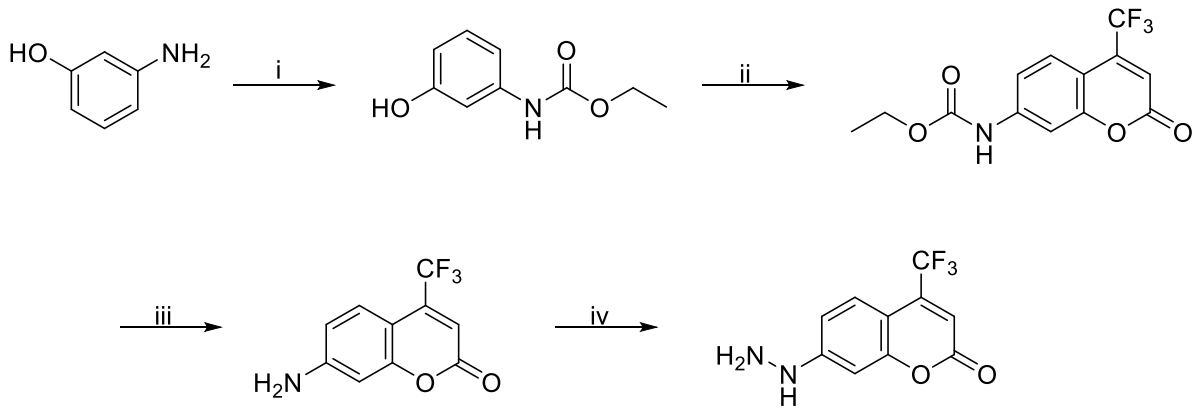

Scheme 1. Synthetic pathway to TFCH. i) ethyl chloroformate in ethyl acetate, reflux, 30 min; ii) ethyl 4,4,4-trifluoroacetoacetate in 3:7 ethanol/H_2SO_4, RT, ON; iii) 3:7 glacial acetic acid/ H_2SO_4, reflux, 4 hrs; iv) conc. HCl, 0 °C – a: $NaNO_2$ (aq), 1.5 hrs b: $SnCl_2$, 1.5 hrs.

Kinetic and Spectroscopic Studies

Three aldehyde reactants—propanal, 3-formyl-tyrosine, and salicylaldehyde—were selected to study the hydrazone formation reaction of TFCH. These reactions yield the conjugates depicted in Figure 15.

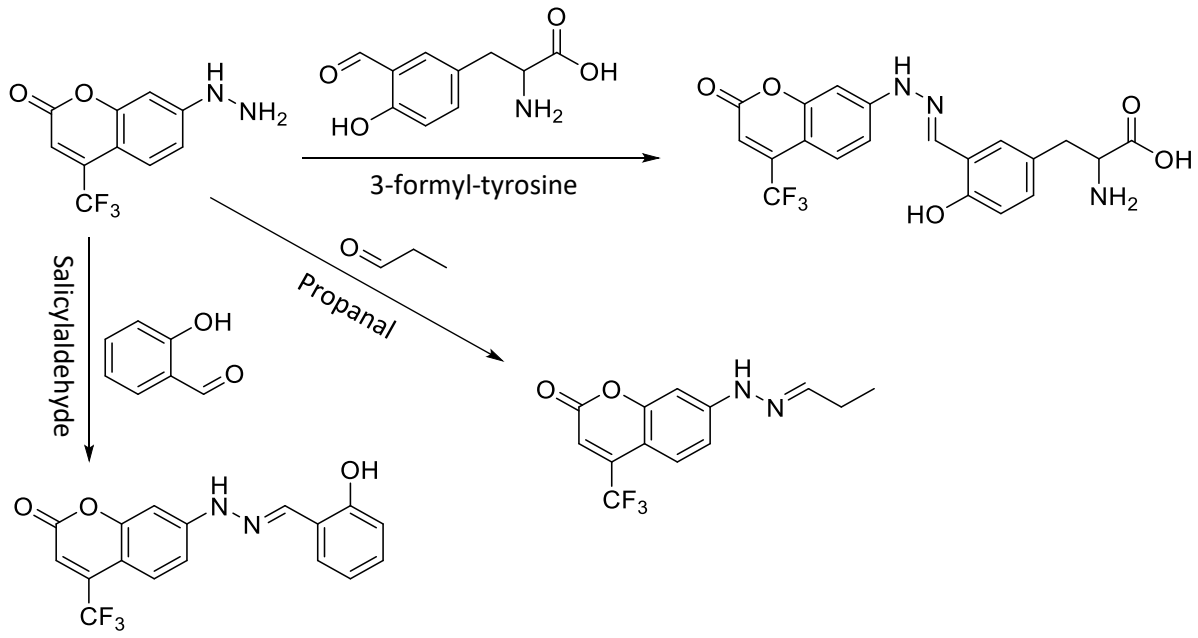

Figure 15. Hydrazone products of TFCH reaction with propanal, 3-formyl-tyrosine, and salicylaldehyde.

The reaction with propanal was first attempted using concentrations of 10 µM TFCH and approximately 140 mM propanal in 100 mM phosphate buffer (pH 7.4). This reaction was completed instantly upon mixing, and the subsequently collected absorbance data showed only a decrease due to the molecule coming out of solution. The propanal concentration was then diluted by a factor of 10, and 10 mM phosphate buffer (pH 7.4) was used, but this reaction was complete in under 30 seconds, and again, the product rapidly came out of solution. The concern

with this observation is that the aggregated species causes a reduction of the enhanced fluorescence signal. This was exemplified by the following attempt, which used 5 µM TFCH and 1.4 mM propanal, and saw the fluorescence enhancement increase from two-fold to four-fold despite the lower reactant concentrations. But this reaction was still not completely free of solubility problems—the kinetics plot (Figure 16) shows a noticeable decline in absorbance beginning at about 600 seconds.

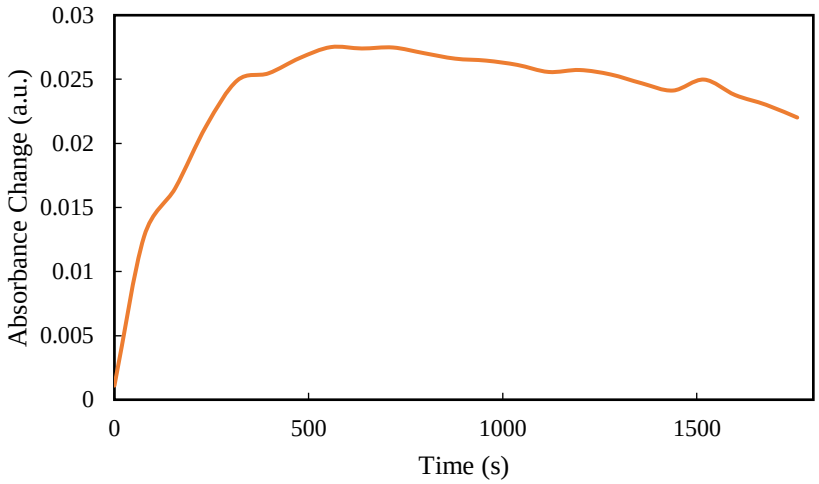

Figure 16. Reaction kinetics of hydrazone formation from TFCH (5 µM) and propanal (1.4 mM). Tracked by absorbance change at 386 nm.

The reaction of TFCH with 3-formyl-tyrosine was tested next to see if the polar amine and carboxylic acid groups on the aldehyde would improve the solubility of the hydrazone conjugate. The goal was to start with a low concentration of 3-formyl-tyrosine and increase it with each trial until aggregation of the product was observed. The first attempt reacted 10 µM TFCH with 100 µM 3-formyl-tyrosine (Figure 17)

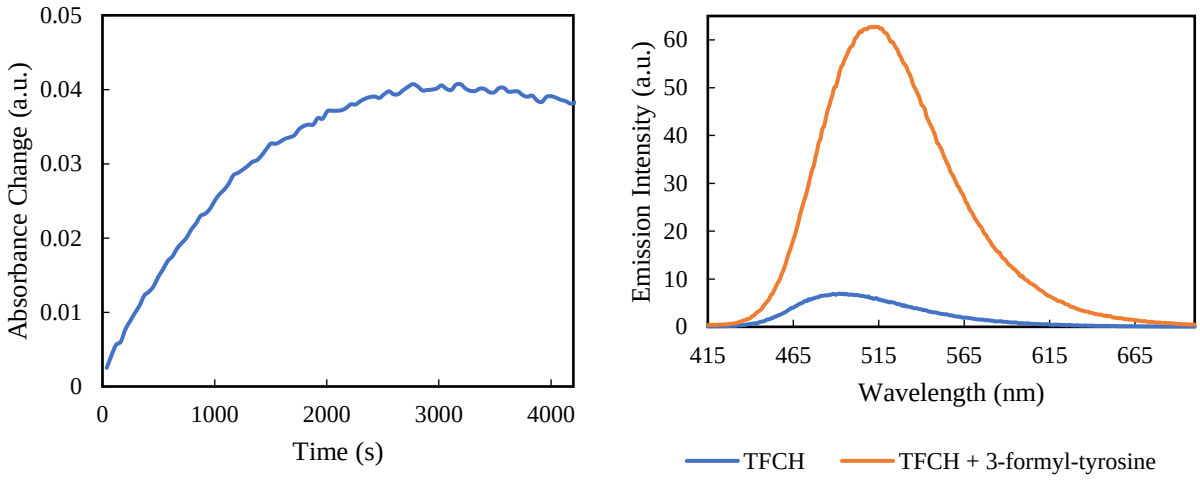

Figure 17. Left: Reaction kinetics, tracked by absorbance change at 423 nm, of hydrazone formation from TFCH (10 µM) and 3-formyl-tyrosine (100 µM) in 10 mM phosphate buffer (pH 7.4). Right: Fluorescence emission spectra (λ_{ex} = 405 nm) from before and after this reaction.

While the emission spectra display nearly 10-fold fluorescence enhancement, 3-formyl-tyrosine was abandoned for two reasons: 1) the UV spectrum of our sample contained unexpected peaks that gradually became lower after dilution (Figure 18; possibly explained by the presence of 3-formyl-tyrosine molecules that had condensed to form imines), potentially influencing the reaction and making it difficult to track by absorbance change; and 2) even at the relatively low concentration of 100 µM, some aggregation is indicated by the absorbance decrease at the tail end of the collected data, and higher concentrations would exacerbate this issue.

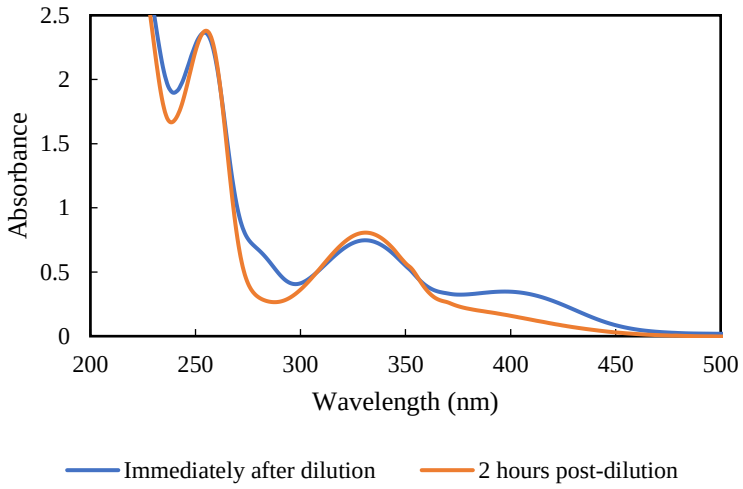

Figure 18. Absorbance spectrum of 3-formyl-tyrosine diluted to 200 µM from solid, collected immediately after and two hours post-dilution.

Still, the reaction was relatively fast, reaching a plateau within an hour. To evaluate the increase in rate afforded by the amino acid component of 3-formyl-tyrosine, the reaction was replicated at the same concentrations using salicylaldehyde, which is equivalent to the side chain of 3-formyl-tyrosine. This reaction (Figure 19) was much slower, appearing to progress but not reaching its plateau within three hours. Expectedly, fluorescence enhancement was also diminished, yielding only a four-fold increase in emission.

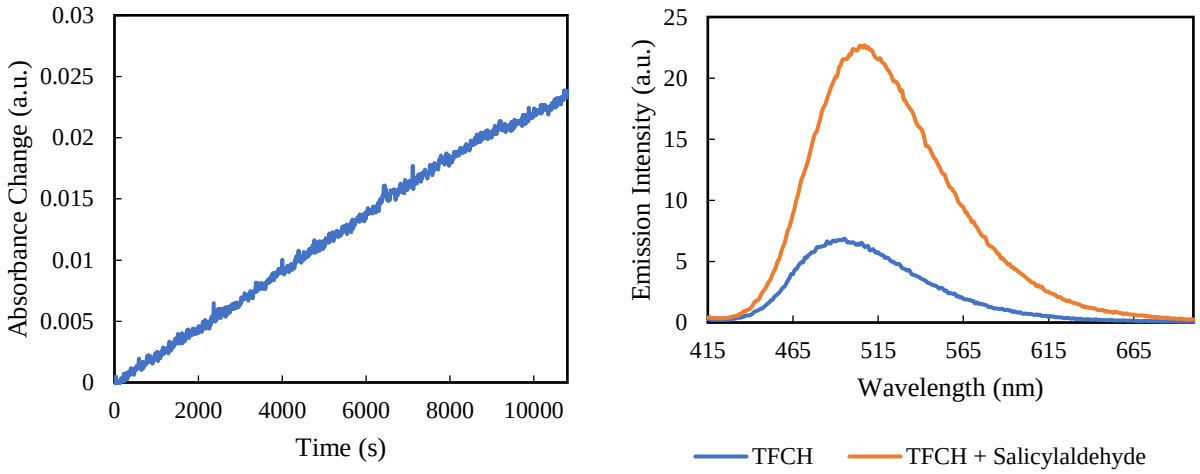

Figure 19. Left: Reaction kinetics, tracked by absorbance change at 274 nm, of hydrazone formation from TFCH (10 µM) and salicylaldehyde (100 µM) in 10 mM phosphate buffer (pH 7.4). Right: Fluorescence emission spectra (λ_{ex} = 405 nm) from before and after this reaction.

Finally, to characterize the photochemical properties of the TFCH-propanal hydrazone, TFCH was reacted with 100-fold excess of propanal. To limit aggregation, the TFCH concentration was limited to 5 µM. The reaction kinetics, as well as the absorbance and emission spectra of the products and TFCH, are depicted in Figure 20. They demonstrate a fast reaction—complete in under 15 minutes—and more than 18-fold fluorescence enhancement. Both these characteristics represent significant advantages compared to the same reaction with JCH.

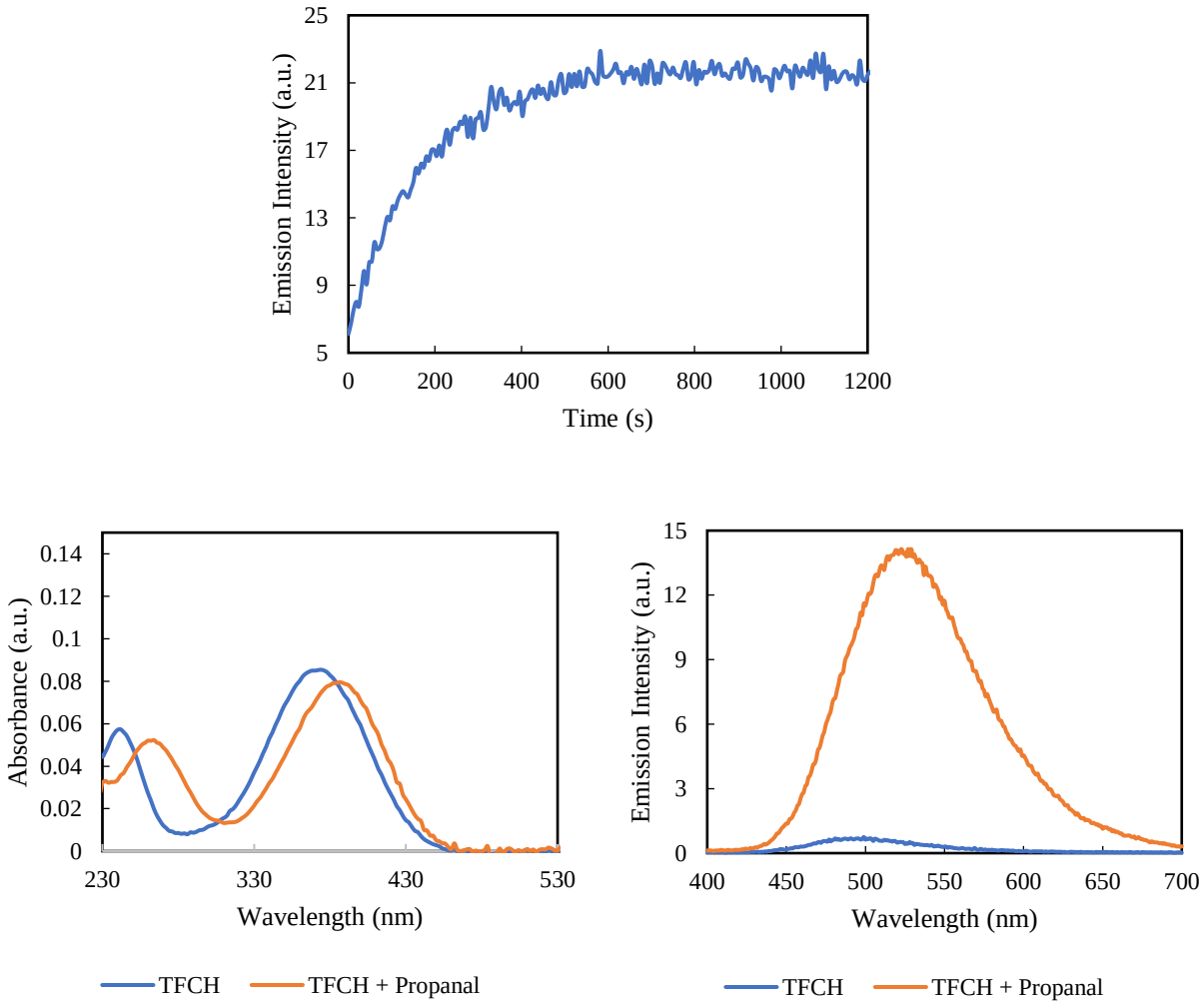

Figure 20. Top: Reaction kinetics, tracked by change in fluorescence emission intensity (λ_{ex} = 388 nm, λ_{em} = 550 nm), of hydrazone formation from TFCH (5 µM) and propanal (500 µM) in 10 mM phosphate buffer (pH 7.4). Bottom left: Absorbance spectra from before and after this reaction. Bottom right: Fluorescence emission spectra (λ_{ex} = 388 nm) before and after reaction.

Table 2 lists the absorbance and emission maxima for TFCH and its propanal-hydrazone conjugate in 10 mM phosphate buffer. As with JCH, both the absorbance and emission maxima of the hydrazone conjugate are red-shifted compared to TFCH. But in contrast to JCH, the emission maximum is shifted further than the absorbance maximum, resulting in an increased

Stokes shift in the hydrazone. For both species, the Stokes shift falls in the approximate range of 125-145 nm, more than double that of JCH.

Table 2. Absorbance and emission maxima of TFCH and the reaction product of TFCH and propanal, in 10 mM phosphate buffer (pH 7.4).

Molecule	Absorbance Maximum (nm)	Emission Maximum (nm)
TFCH	374	499
TFCH + Propanal	386	529

Stability Studies

Given that TFCH is now used by our lab and others as a visualization tool, there is a need to establish the long-term stability of the molecule. This is especially important if it might be degraded into other fluorescent species. To this end, a stock solution of TFCH in DMSO that had sat at room temperature for over a year ("old") was obtained and was compared to a fresh solution prepared from the pure solid ("new"). The solutions were diluted to 5 μM in 10 mM phosphate buffer (pH 7.4) and were each reacted with 1.4 mM of propanal. The kinetics plots, as well as the emission spectra from before and after the reaction are depicted in Figure 21. The emission spectra from before the reaction show a fluorescence that is about twice as high in the old sample, compared to the new sample. Moreover, despite the kinetics plots appearing similar, the fluorescence of the product from the old is noticeably bluer than that from the new. Altogether, these results suggest the presence of highly fluorescent degradation products.

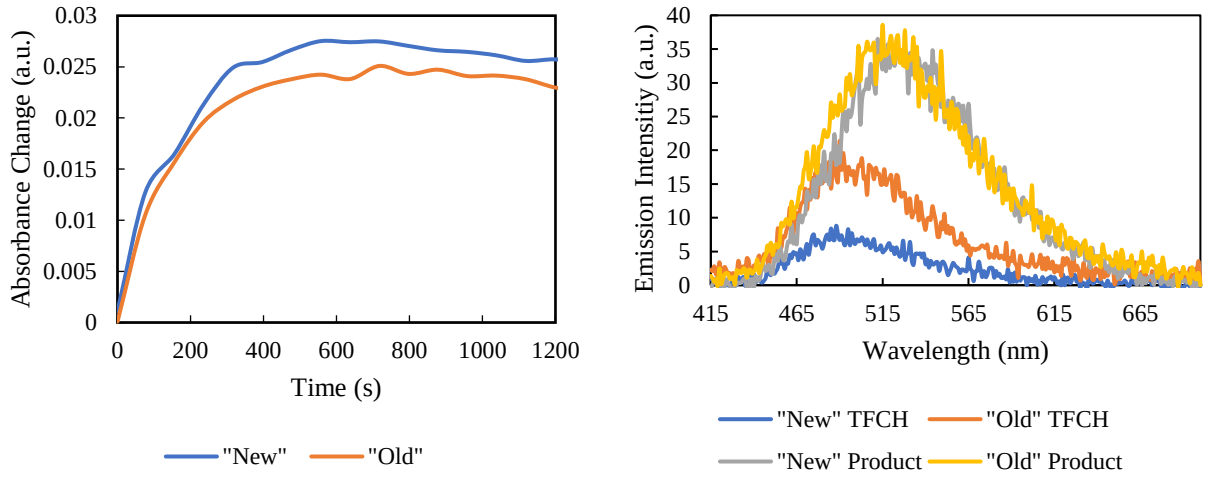

Figure 21. Left: Reaction kinetics, tracked by absorbance change at 386 nm, of hydrazone formation from "old" and "new" TFCH (5 µM) and propanal (1.4 mM) in 10 mM phosphate buffer (pH 7.4). Right: Fluorescence emission spectra (λ_{ex} = 405 nm) from before and after these reactions.

In light of this finding, the stability of TFCH under standard recommended storage conditions for similar fluorescent probes (solution in DMSO, frozen at −20 °C, and protected from light) was assessed. A fresh stock solution of TFCH in DMSO was prepared from the solid, and emission spectra were collected before and after reaction (of 10 µM) with propanal (500 µM) in 10 mM phosphate buffer (pH 7.4). The sample was then subjected to 20 freeze-thaw cycles where it was allowed to warm to room temperature each time, and the experiment was repeated. The spectra (Figure 22) show no notable differences, demonstrating the stability of TFCH under the tested conditions.

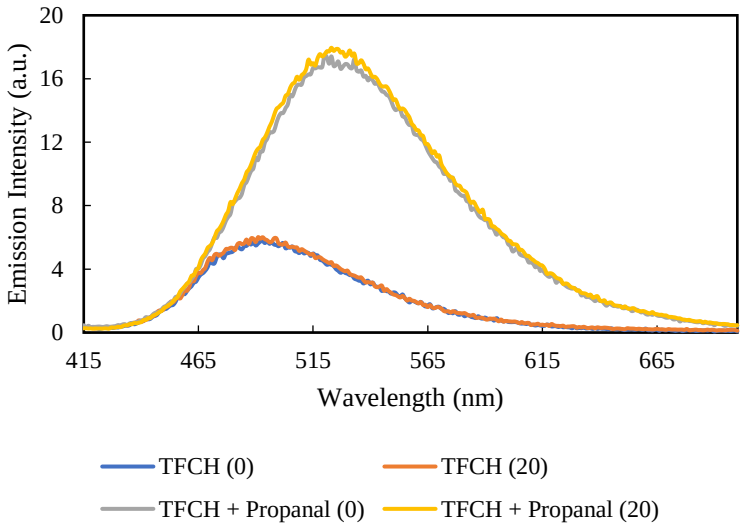

Figure 22. Fluorescence emission spectra (λ_{ex} = 405 nm) from before and after the reaction of TFCH (10 µM) with propanal (500 µM), for TFCH solutions prepared from a freshly made stock (0) and from the same stock after 20 freeze-thaw cycles.

Coumarin Acid Hydrazine (CAH)

The initial goal was to add to our lab's library of coumarin-based probes by synthesizing and characterizing a coumarin hydrazine derivative substituted with an ester at the 4-position. Considering the familiar obstacle of aggregation, the synthetic intermediate with a carboxylic acid at this position (Coumarin Acid Hydrazine; CAH; Figure 23) was also predicted to be of potential value, due to the increased water solubility the functional group might provide.

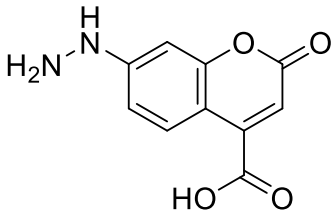

Figure 23. Structure of CAH

Scheme 2 outlines the route taken to synthesize CAH. Obtaining the ester would require an additional esterification step. Significant challenges were encountered when trying to apply a modified form of the TFCH synthetic scheme to reach CAH. Specifically, the work-ups for each of the last three steps needed considerable adjustment. Because of this, and ultimately, because of time constraints, only a very small amount of CAH was synthesized, and the ester was not made.

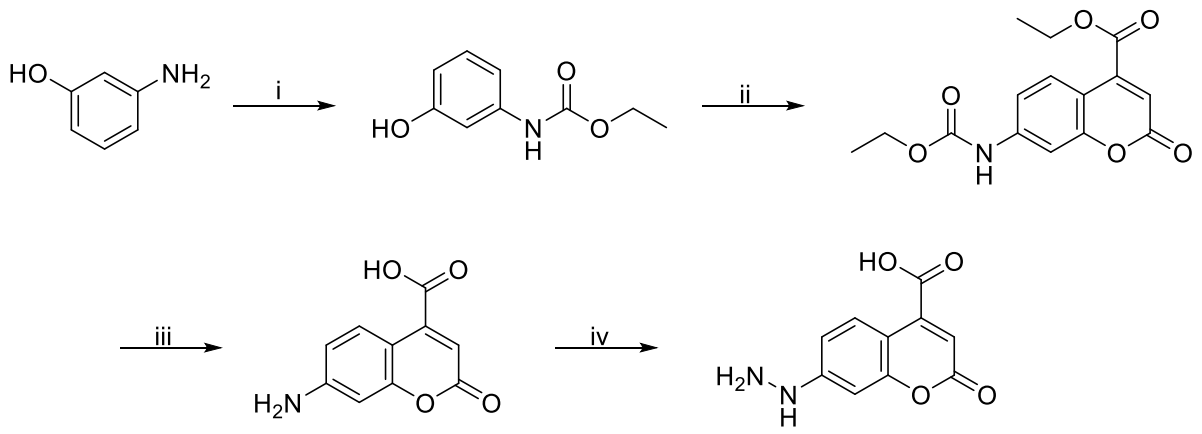

Scheme 2. Synthetic pathway to CAH. i) ethyl chloroformate in ethyl acetate, reflux, 30 min; ii) diethyl oxaloacetate sodium salt in 3:7 ethanol/H_2SO_4, RT, 4 hrs; iii) 3:4 glacial acetic acid/ H_2SO_4, reflux, 4 hrs; iv) 1:1 conc. HCl/H_2O, 0 °C – a: $NaNO_2$ (aq), 1.5 hrs b: $SnCl_2$, 1.5 hrs.

The first step—protection of 3-aminophenol—was completed several times without issue and with high yields. But in the second step, an ice water quench following the cyclization reaction did not produce a precipitate, as it does for the analogous intermediate of the TFCH synthesis. On first attempt, this issue was addressed by extracting the reaction mixture with ethyl acetate, but while this did yield the expected coumarin, it brought through a considerable

quantity of impurities along with it. Regardless, the deprotection step was attempted using this material. Again, the proposed work-up procedure—precipitation by basification—did not yield a precipitate. Here, this should have been expected, as the desired product of the deprotection contains both an amine and a carboxylic acid, and is thus a zwitterion in its neutral form and ionized at any pH. A solid product was obtained by evaporation, but it was primarily composed of salts from both the previous steps. Although ^{1}H NMR gave a weak signal consistent with the intermediate, the material was deemed too impure to use in the diazotization.

To avoid the issues that were encountered in the first two steps, an unprotected ester substituted coumarin amine was targeted directly by reaction of 3-aminophenol and diethyl oxalacetate. This reaction had been reported in the literature with good yields and no purification necessary beyond work-up.[9] If successful, the intermediate could be directly carried through to the diazotization/reduction to yield CAH (the ester would be hydrolyzed under the reaction conditions). But two trials failed to yield the pure product—^{1}H NMR gave a messy spectrum in the aromatic region, and TLC indicated the presence of at least five fluorescent products.

At this point, the original scheme was revisited, beginning with the cyclization. After much trial and error, the product was purified by basification of the reaction mixture, extraction with ethyl acetate, column chromatography with 1:1 ethyl acetate/hexanes, and trituration in petroleum ether. The yield was 3.6 percent. This process was repeated, and trituration became unnecessary when 3:5 ethyl acetate/hexanes was used for the column. The yield was 9.5 percent, and was likely still this low because the reaction was stopped too early (TLC used to track reaction progress was misread) and because only 2 equivalents of diethyl oxalacetate were used (rather than 3). Running the reaction longer and following the revised procedure should provide

satisfactory yields in the future. The absorption and fluorescence emission spectra of this protected aminocoumarin ester intermediate are shown in Figure 24.

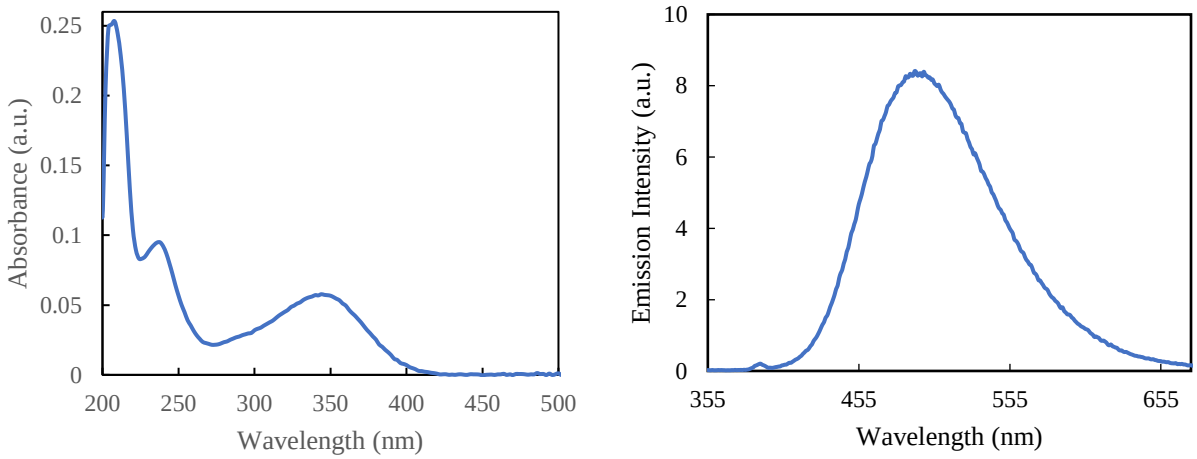

Figure 24. Absorption (left) and fluorescence emission (right; λ_{ex} = 344 nm) spectra, collected in phosphate buffer (pH 7.4), of the protected aminocoumarin ester intermediate in the synthesis of CAH.

To avoid the problem caused by the zwitterionic character of the deprotected and hydrolyzed intermediate, the hydrolysis was attempted by heating the protected aminocoumarin under the solvent conditions of diazotization (concentrated HCl), so it could be carried through to the next step in one pot. But this yielded minimal conversion, even when refluxed overnight. The protected amine was recovered by boiling off most of the solvent, cooling the solution, and collection by vacuum filtration. The deprotection was then retried using the originally proposed solvent (H_2SO_4). This reaction was nearly complete within 30 minutes, highlighting the need for a very strong acid in removing this particular protecting group. After quenching the reaction with a small amount of water, the product was isolated by extraction with methyl ethyl ketone under acidic conditions. Methyl ethyl ketone was selected because it is relatively polar but still immiscible with water, and conditions were kept acidic because a test extraction revealed that

significantly more product moved into the aqueous layer as it was brought closer to neutral pH. The absorption and fluorescence emission spectra of this deprotected aminocoumarin carboxylic acid intermediate are shown in Figure 25.

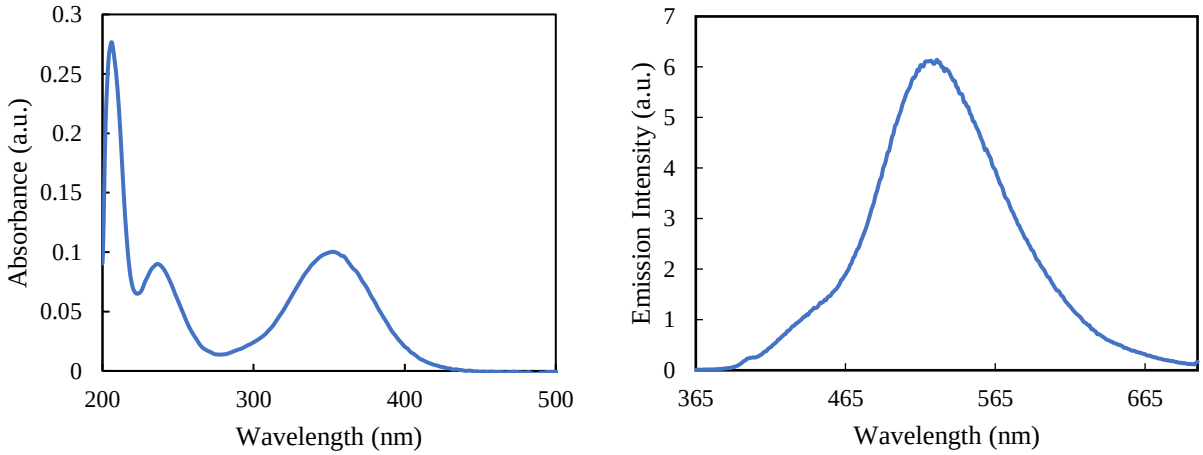

Figure 25. Absorption (left) and fluorescence emission (right; λ_{ex} = 352 nm) spectra, collected in phosphate buffer (pH 7.4), of the aminocoumarin carboxylic acid intermediate in the synthesis of CAH.

Overall, only a small amount of deprotected aminocoumarin was available for the diazotization/reduction. Moreover, it was very prone to adhesion due to static electricity and was difficult to transfer between flasks. The final step was thus attempted on a very small scale. The starting material did not dissolve in concentrated hydrochloric acid, even with heating, stirring, added volume and time. Distilled water was added, and all material was dissolved when a 1:1 ratio of concentrated hydrochloric acid to water was reached. As desired, a precipitate was obtained, but the particle size was too small for collection by filtration. Instead, it was collected by centrifugation and dissolved in ethanol, which was then evaporated off. The ^{1}H NMR spectrum of this solid gave broad and non-distinctive peaks in the coumarin aromatic region, which has been observed as an effect of residual salts in similar coumarin hydrazine products

(like TFCH). After a failed trial in ethanol, recrystallization from isopropanol was successful, and the ^{1}H NMR spectrum of the crystals (Appendix) was consistent with the structure of CAH, and showed no signal for the amine starting material.

The initial UV spectrum (Figure 26) of this material showed a saturating absorbance from 200-300 nm (likely caused by salts), leaving the entire spectrum unreadable. LC-MS did not find the molecular ion for CAH and did not detect any absorbance beyond 300 nm, despite the readily visible absorbance of the solution. The material was cleaned by extraction with methyl ethyl ketone from aqueous solution, and readable absorption and fluorescence spectra (Figure 26) were directly obtained using extract. These spectra resemble those of the amine analogue, as would be expected for CAH. There is a slight blue-shift, but this is likely attributable to the decreased polarity of methyl ethyl ketone, compared to phosphate buffer.

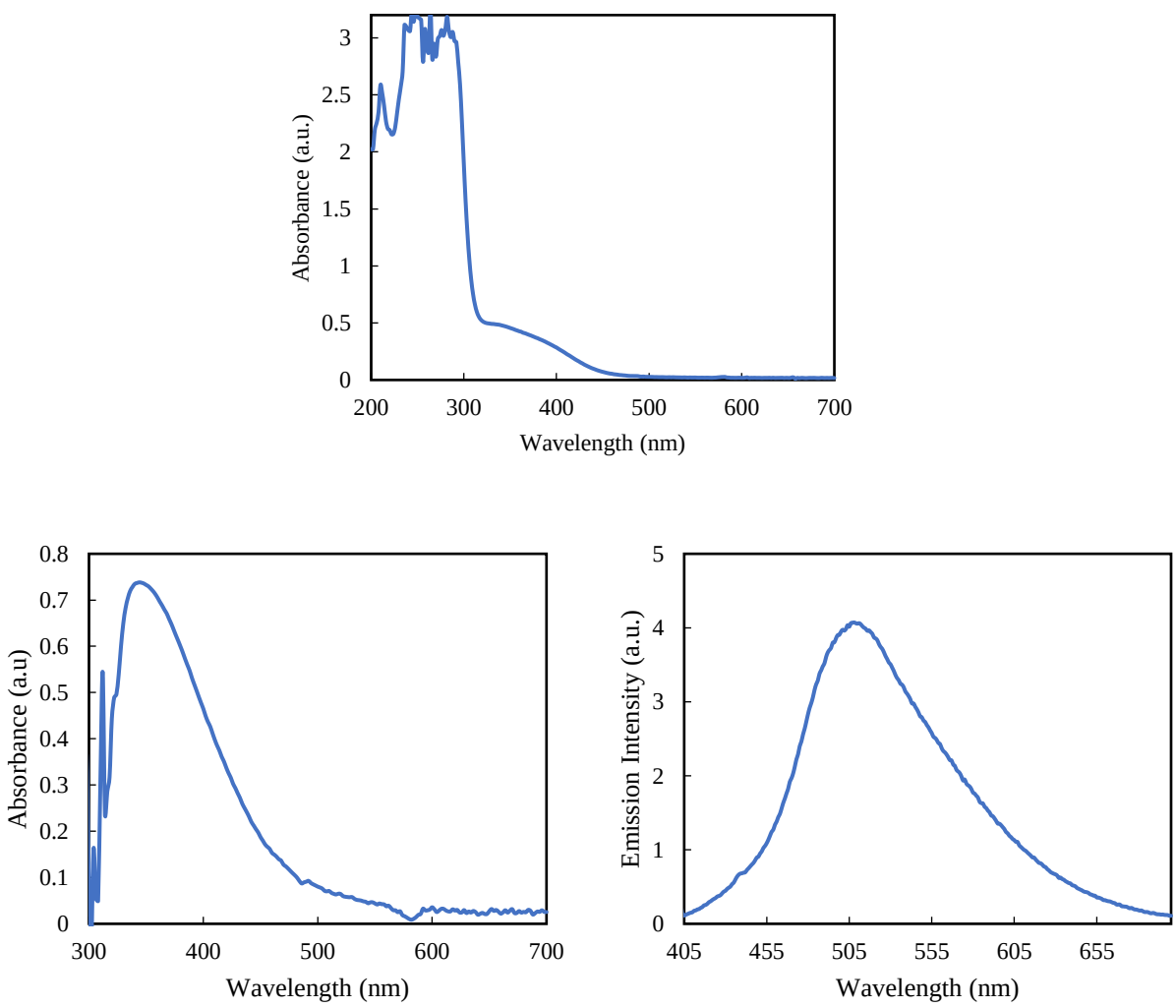

Figure 26. Top: Absorbance spectrum of recrystallized diazotization/reduction product in phosphate buffer (pH 7.4). Bottom left: Absorbance spectrum of a methyl ethyl ketone extraction of the phosphate buffer solution (absorbances below 300 are lost due to the blank signal of methyl ethyl ketone, which absorbs in this region). Bottom right: Fluorescence emission spectrum of the methyl ethyl ketone extract (λ_{ex} = 344 nm)

But even with this cleaner material, LC-MS did not detect CAH or any absorbance above 300 nm. Under the applied parameters, LC-MS is apparently incompatible with the synthesized material (attempted as a control, TFCH was also not detected). Without this data, it is still reasonable to conclude that CAH was made. LC-MS and NMR gave distinctive signals for the

synthetic intermediates, and none of these were observed for the diazotization/reduction product, thus ruling out their presence. The NMR spectrum (Appendix) is also inconsistent with the diazonium salt intermediate and the potential diazotization by-product in which the diazonium salt is lost. Additionally, it shows peaks consistent with the NH protons of a hydrazine salt (downfield singlets for NH and NH_3^+). Finally, the absorbance and fluorescence spectra are consistent with expectations for CAH based on the spectra for the amine starting material. This conclusion must be made with the caveat that it is not entirely definite. Ultimately, time constraints and a shortage of material prevented any further tests, which therefore remain for future work.

Conclusions and Future Work

JCH and TFCH

The comparison of the two probes revealed that TFCH has preferable properties for most applications inside cells. TFCH reacts faster, has a larger Stokes shift, and a yields a much greater fluorescence enhancement upon conjugation in aqueous solvent, compared to JCH. Still, the redder absorbance of JCH (among other potential advantages) may lead to its eventual application, and the catalytic methods explored here will aid in achieving faster reactions and better fluorescence enhancement. As for TFCH, for all three tested aldehydes, the conjugates began to come out of solution above 5 μM, suggesting that concentrations should be kept at or below this level, and presenting a potential limitation to practical use of the molecule.

Future work should assess the same reactions in a more quantitative manner, using the data to establish rate and equilibrium constants. Reactions with other aldehydes, and specifically those found as products of protein carbonylation, should also be examined outside cells, to determine if the probes react with any of them preferentially when present in combination within cells. Finally, the mechanism underlying the elevated fluorescence of JCH in aqueous solvent should be explored, and the highly fluorescent degradation products of TFCH should be identified.

CAH

The proposed synthetic route to CAH was successfully implemented to obtain the protected aminocoumarin ester and the aminocoumarin carboxylic acid intermediates. CAH was most likely obtained as well, although the diazotization/reduction product could not be sufficiently characterized to yield a definite positive identification.

Future work should make use of the difficulties and optimizations noted here—and should engage in further optimization—in replicating the reported synthesis. The first priority for building on this project is obtaining enough CAH for thorough characterization of purified material. After this, its suitability as a probe for use inside cells should be assessed. Furthermore, the ester analog can be made by esterification of CAH and should be similarly characterized and evaluated as a probe. Finally, research can attempt to link drugs or other molecules of interest, such as a PROTAC, at the ester function.

Synthesis

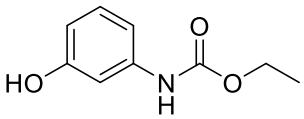

Ethyl (3-hydroxyphenyl)carbamate

In a dried flask, 5.36 g (49.1 mmol) of 3-aminophenol was dissolved in 53 mL of ethyl acetate. The solution heated to reflux in an 85 °C oil bath. After 30 minutes of reflux, 2.3 mL (18.9 mmol) of ethyl chloroformate was added dropwise with a syringe. Precipitation was noted immediately, and the solution was refluxed for another 30 minutes, after which it was removed from heat and allowed to cool to room temperature. The precipitate was removed by vacuum filtration, the filtrate was collected, and solvents were evaporated under vacuum to give 4.34 g (100%) of ethyl (3-hydroxyphenyl)carbamate, an off-white solid.

^{1}H ($CDCl_3$): δ 1.294 (t, 3H, J = 7.11, 7.11), 4.207 (q, 2H, J = 7.08, 7.08, 7.08), 6.5324 (dd, 1H, J = 2.44, 8.07, 2.44), 6.5629 (broad s, 1H), 6.6858 (d, 1H, J = 8.03), 7.1201 (t, 2H, J = 8.09, 8.09), 7.2140 (broad s, 1H).

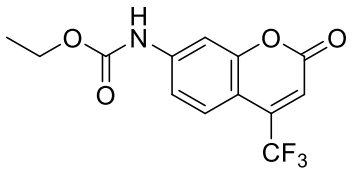

Ethyl (2-oxo-4-(trifluoromethyl)-2*H*-chromen-7-yl)carbamate

A dried flask containing 1.01 g (5.58 mmol) of the starting material [ethyl (3-hydroxyphenyl)carbamate] was placed in an ice bath. To this, 4.5 mL of ethanol was added, followed by 10.5 mL of sulfuric acid, and the solution was stirred. Once all starting material had dissolved, 2.44 mL (17 mmol) of ethyl 4,4,4-trifluoroacetoacetate was added dropwise with a syringe. The reaction was stirred overnight, after which it was quenched with ice water, causing precipitation. This precipitate was collected by vacuum filtration, rinsed with ice water, and dried under vacuum, yielding 0.336 g (20%) of the target molecule, a pale yellow solid.

^{1}H (DMSO-d6): δ 1.277 (t, 3H, J = 7.11, 7.11), 4.1925 (q, 2H, J = 7.09, 7.09, 7.09), 6.8764 (s, 1H), 7.4966 (dd, 1H, J = 1.89, 6.95, 2.07), 7.6507 (d, 1H, J = 1.75), 7.6801 (d, 1H J = 1.95), 10.3385 (s, NH).

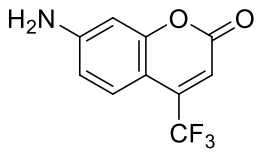

7-amino-4-(trifluoromethyl)-2*H*-chromen-2-one

A 0.795 g (2.64 mmol) portion of the starting material [ethyl (2-oxo-4-(trifluoromethyl)-2H-chromen-7-yl)carbamate] was dissolved in 2 mL of glacial acetic acid, followed by careful addition of 4.5 mL of sulfuric acid. The flask was placed in a 150 °C oil bath and brought to reflux. After four hours, the solution was removed from heat and quenched with approximately 20 mL of ice water. To neutralize the solution, saturated NaOH was added dropwise until precipitation stopped. The precipitate was collected by vacuum filtration, rinsed with ice water, and dried under vacuum, yielding 0.414 g (68%) of the target molecule, a bright yellow solid.

^{1}H (DMSO-d6): δ 6.4519 (s, 1H), 6.5043 (d, 1H, J = 2.12), 6.5238 (broad s, NH_2), 6.6502 (dd, 1H, J = 2.18, 6.68, 2.18), 7.3615 (dd, 1H, J = 2.19, 6.73, 2.07).

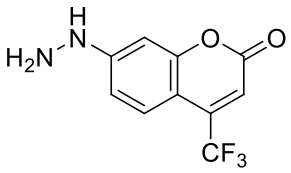

7-hydrazineyl-4-(trifluoromethyl)-2*H*-chromen-2-one

In a dried three-necked flask with an attached thermometer, 0.412 g (1.80 mmol) of the starting material [7-amino-4-(trifluoromethyl)-2*H*-chromen-2-one] was dissolved in 10 mL of concentrated hydrochloric acid. The solution was brought below 0 °C and this temperature was maintained throughout the reaction. Reactant solutions were prepared by dissolving 0.157 g (2.27 mmol) of sodium nitrite in 1 mL of distilled water and 1.30 g (5.86 mmol) of stannous chloride dihydrate in 1.5 mL of concentrated hydrochloric acid, and these were also brought below 0 °C in the ice bath. The sodium nitrite solution was added dropwise to the reaction flask, with care taken to keep the reaction temperature below zero. After 1.5 hours, the stannous chloride solution was added in the same manner. Another 1.5 hours later, the flask was removed from the ice bath and allowed to reach room temperature. Its contents were then filtered through a Büchner funnel with a fritted glass filter. The precipitate was collected by vacuum filtration, rinsed with ice water, and dried under vacuum, yielding 0.207 g (41%) of the target molecule, a pale yellow-brown solid, as the hydrochloride salt.

^{1}H (DMSO-d6): δ 6.7357 (s, 1H), 6.8813 (d, 1H, 2.01), 6.9257 (dd, 1H, J = 2.10, 6.75, 2.15), 7.5788 (d, 1H, 7.67), 8.9682 (broad s, NH).

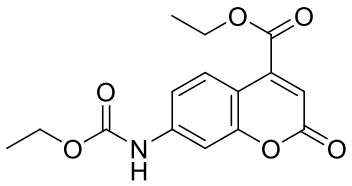

Ethyl 7-((ethoxycarbonyl)amino)-2-oxo-2*H*-chromene-4-carboxylate

A 4.34 g (23.9 mmol) portion of the starting material [ethyl (3-hydroxyphenyl)carbamate] was dissolved in 19.5 mL of ethanol, followed by careful addition of 45.6 mL of sulfuric acid. The solution was cooled by placing the flask in an ice water bath. A total of 10.1 g (48.5 mmol) of solid diethyl oxalacetate sodium salt was added in small portions, waiting for dissolution between each. The reaction was stirred at room temperature for 3.5 hours (note: letting the reaction run longer may give a better yield), after which the reaction mixture was quenched with ice water, made basic by dropwise addition of saturated NaOH, and extracted with ethyl acetate. Solvents were removed under vacuum, and the product was purified by silica column chromatography using 3:5 ethyl acetate/hexanes as the mobile phase. After evaporation of the purified fractions, 0.695 g (9.5%) of the target molecule was obtained as a salmon-colored solid.

^{1}H (DMSO-d6): δ 1.2751 (t, 3H, 7.15, 7.05), 1.3589 (t, 3H, 7.15, 7.13), 4.1871 (q, 2H, 7.09, 7.09, 7.09), 4.4033 (q, 2H, 7.09, 7.13, 7.09), 6.7157 (s, 1H), 7.4307 (dd, 1H, 2.01, 6.79, 2.21), 7.6289 (d, 1H, 2.02), 8.0000 (d, 1H, 8.84), 10.2470 (s, NH)

^{13}C (DMSO-d6): δ 14.307, 14.846, 61.291, 62.776, 105.156, 110.423, 115.157, 115.820, 127.656, 143.260, 143.884, 153.770, 155.256, 160.061, 164.226

MS: 306 m/z $[M+H]^{+}$

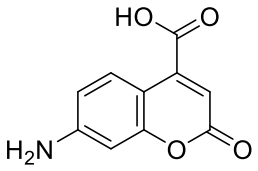

7-amino-2-oxo-2*H*-chromene-4-carboxylic acid

In a dried flask, 0.500 g (1.64 mmol) of the starting material [ethyl 7-((ethoxycarbonyl)amino)-2-oxo-2*H*-chromene-4-carboxylate] was dissolved in 4 mL glacial acetic acid, followed by addition of 5 mL sulfuric acid. The reaction solution was heated to reflux using a 126 °C oil bath. After 6.5 hours of reflux, the reaction was quenched with 10 mL of ice water. The solution was basified slightly by dropwise addition of saturated NaOH and was then extracted with methyl ethyl ketone. The extract was washed once with brine and solvents were removed under vacuum, giving 0.154 g (44%) of the target molecule, a red solid.

^{1}H (DMSO-d6): δ 6.2852 (s, 1H), 6.3233 (broad s, NH_2), 6.4569 (d, 1H, 2.07), 6.5889 (dd, 1H, 1.89, 6.89, 2.11), 7.7563 (d, 1H, 8.78)

^{13}C (DMSO-d6): δ 99.195, 105.173, 109.279, 112.205, 128.129, 145.499, 153.979, 156.985, 161.107, 166.522

MS: 206 m/z $[M+H]^+$

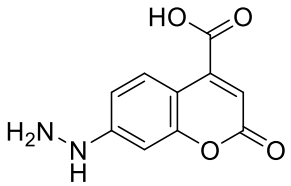

7-hydrazineyl-2-oxo-2*H*-chromene-4-carboxylic acid

In a dried three-necked flask with an attached thermometer, 0.080 g (0.39 mmol) of the starting material [7-amino-2-oxo-2*H*-chromene-4-carboxylic acid] was dissolved in 22 mL of a solution containing a 6:5 mixture of concentrated hydrochloric acid and distilled water. The solution was brought below 0 °C and this temperature was maintained throughout the reaction. Reactant solutions were prepared by dissolving 0.032 g (0.47 mmol) of sodium nitrite in 0.5 mL of distilled water and 0.282 g (1.24 mmol) of stannous chloride dihydrate in 1 mL of concentrated hydrochloric acid, and these were also brought below 0 °C in the ice bath. The sodium nitrite solution was added dropwise to the reaction flask, with care taken to keep the reaction temperature below zero. After 1.5 hours, the stannous chloride solution was added in the same manner. Another 1.5 hours later, the flask was removed from the ice bath and allowed to reach room temperature. The solution was centrifuged and decanted, and this was repeated with a 5 mL distilled water wash. The solid was then dissolved in ethanol and transferred to a flask, after which the ethanol was removed under vacuum. The obtained solid was recrystallized from isopropanol, yielding a very small amount of light brown crystals.

^{1}H (DMSO-d6): δ 7.0888 (d, 1H, 7.85), 7.2636 (dd, 1H, 2.55, 6.20, 2.55), 7.3732 (s, 1H), 7.4100 (d, 1H, 8.58), 8.2153 (s, 1H), 10.1959 (s, NH_3^+)

References

(1) Lowe F. *Biomarkers of Oxidative Stress*; Springer-Verlag Berlin Heidelberg, 2014.

(2) Dalle-Donne, I.; Aldini, G.; Carini, M.; Colombo, R.; Rossi, R.; Milzani, A. Protein Carbonylation, Cellular Dysfunction, and Disease Progression. *Journal of cellular and molecular medicine* **2006**, *10* (2), 389–406. https://doi.org/10.1111/j.1582-4934.2006.tb00407.x.

(3) Yan, L.-J.; Forster, M. J. Chemical Probes for Analysis of Carbonylated Proteins: A Review. *Journal of Chromatography B* **2011**, *879* (17-18), 1308–1315. https://doi.org/10.1016/j.jchromb.2010.08.004.

(4) Mukherjee, K.; Chio, T. I.; Sackett, D. L.; Bane, S. L. Detection of Oxidative Stress-Induced Carbonylation in Live Mammalian Cells. *Free Radical Biology and Medicine* **2015**, *84*, 11–21. https://doi.org/10.1016/j.freeradbiomed.2015.03.011.

(5) Mukherjee, K.; Chio, T. I.; Gu, H.; Sackett, D. L.; Bane, S. L.; Sever, S. A Novel Fluorogenic Assay for the Detection of Nephrotoxin-Induced Oxidative Stress in Live Cells and Renal Tissue. *ACS Sensors* **2021**, *6* (7), 2523–2528. https://doi.org/10.1021/acssensors.1c00422.

(6) Liu, Xiaogang, et al. “Molecular Design of UV–Vis Absorption and Emission Properties in Organic Fluorophores: Toward Larger Bathochromic Shifts, Enhanced Molar Extinction Coefficients, and Greater Stokes Shifts.” *The Journal of Physical Chemistry C*, vol. 117, no. 32, Aug. 2013, pp. 16584–16595, 10.1021/jp404170w.

(7) Bond, M. J.; Crews, C. M. Proteolysis Targeting Chimeras (PROTACs) Come of Age: Entering the Third Decade of Targeted Protein Degradation. *RSC Chemical Biology* **2021**, *2*, 725–742. https://doi.org/10.1039/d1cb00011j.

(8) Sorrentino, A. Bioorthogonal Development of Reactive Coumarin Based Fluorescent Probes for the Site-Specific Labeling of Biomolecules. Honors Thesis, Binghamton University, 2015.

(9) Besson, T.; Coudert, G.; Guillaumet, G. Synthesis and Fluorescent Properties of Some Heterobifunctional and Rigidized 7-Aminocoumarins. *Journal of Heterocyclic Chemistry* **1991**, *28* (6), 1517–1523. https://doi.org/10.1002/jhet.5570280608.

Appendix

1H NMR Spectrum of ethyl (3-hydroxyphenyl)carbamate

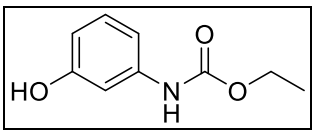

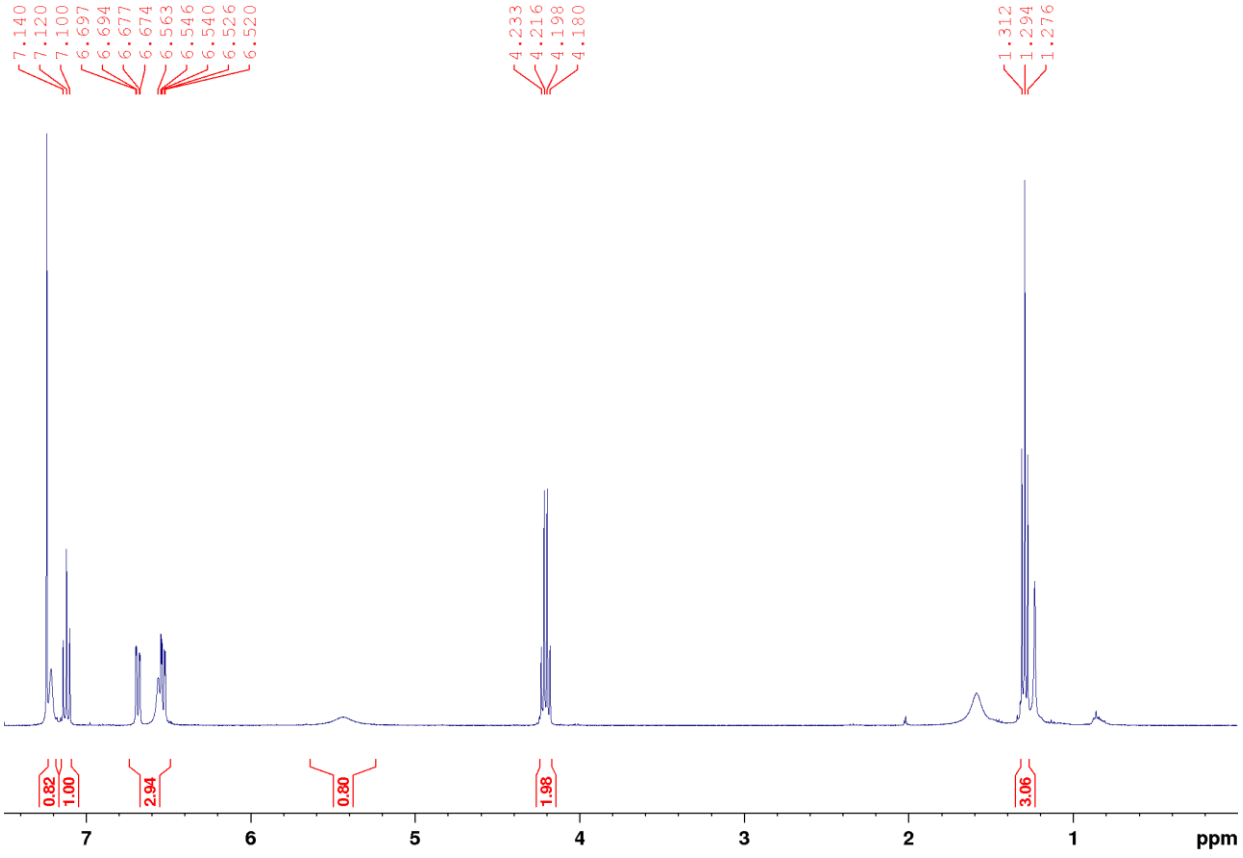

1H NMR Spectrum of ethyl (2-oxo-4-(trifluoromethyl)-2*H*-chromen-7-yl)carbamate

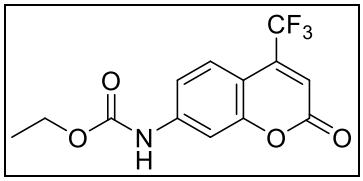

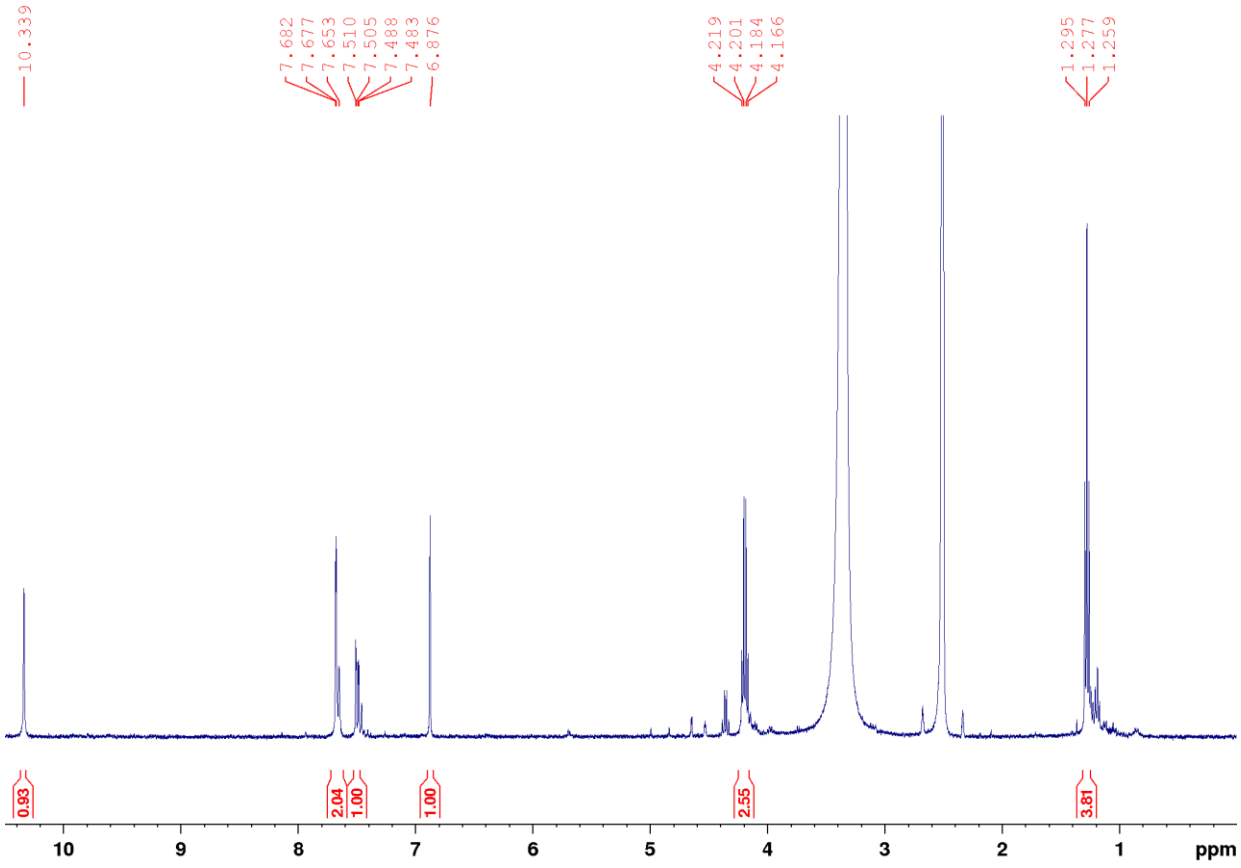

COSY NMR Spectrum of ethyl (2-oxo-4-(trifluoromethyl)-2*H*-chromen-7-yl)carbamate

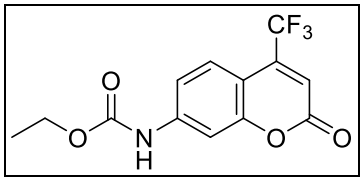

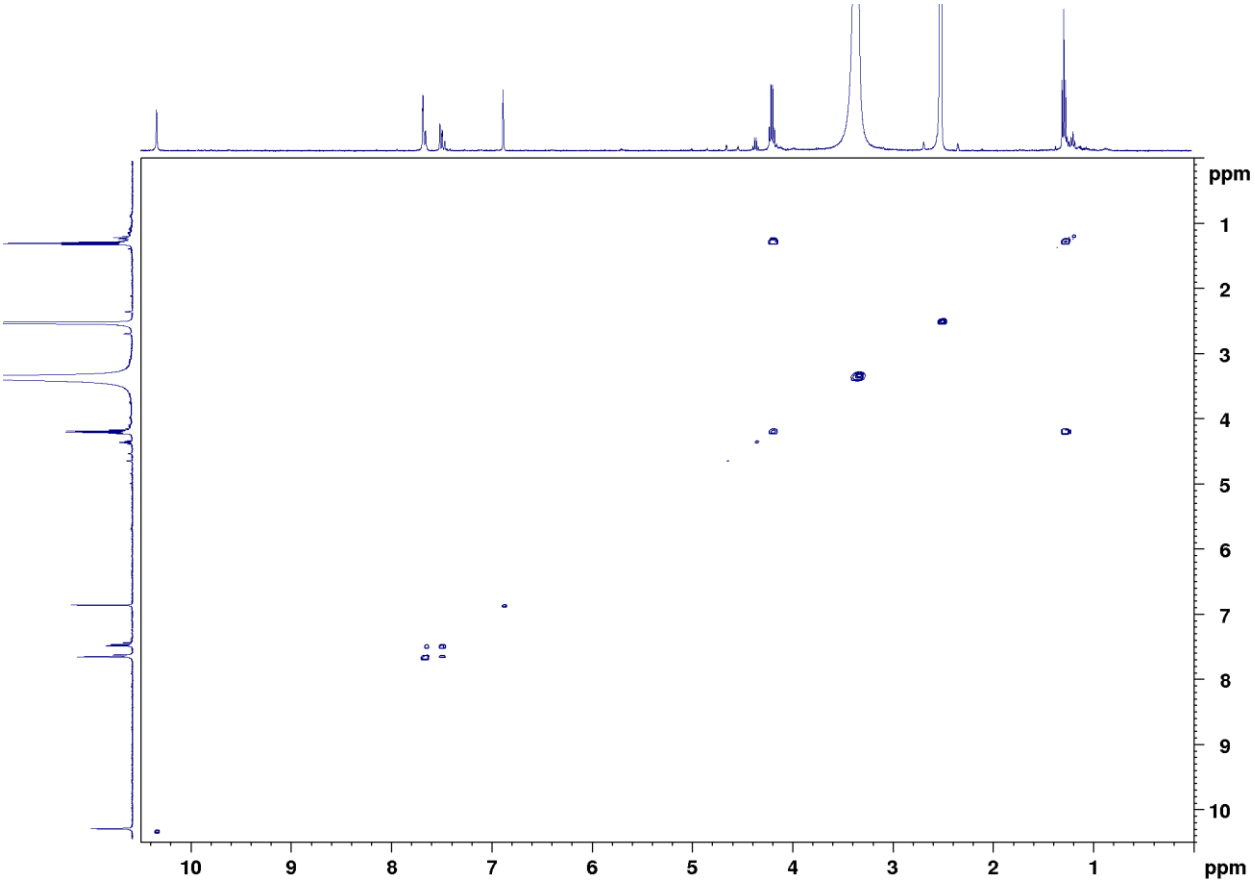

1H NMR Spectrum of 7-amino-4-(trifluoromethyl)-2*H*-chromen-2-one

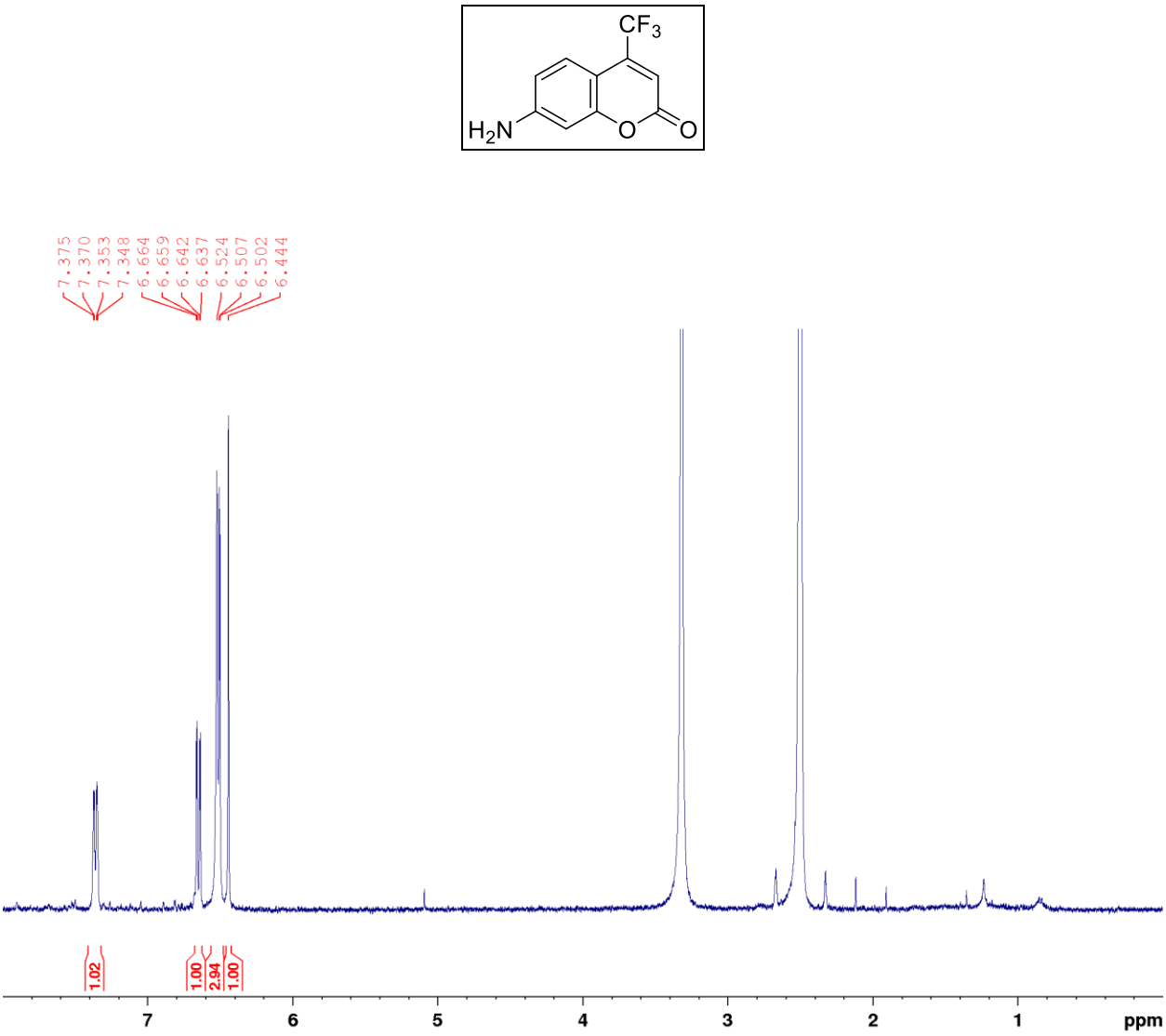

COSY NMR Spectrum of 7-amino-4-(trifluoromethyl)-2*H*-chromen-2-one

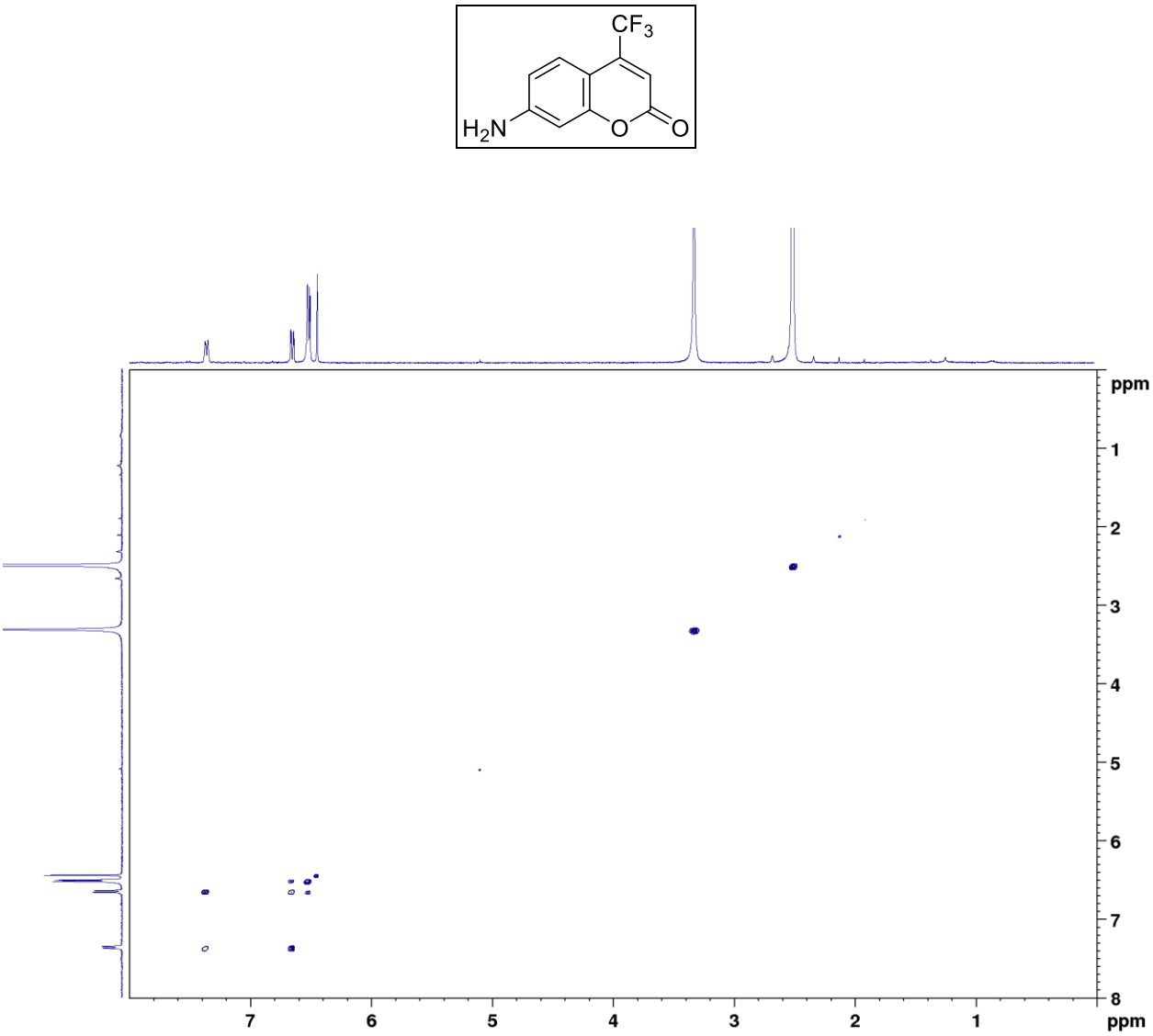

1H NMR Spectrum of 7-hydrazineyl-4-(trifluoromethyl)-2*H*-chromen-2-one (TFCH)

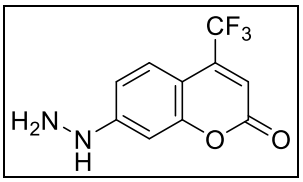

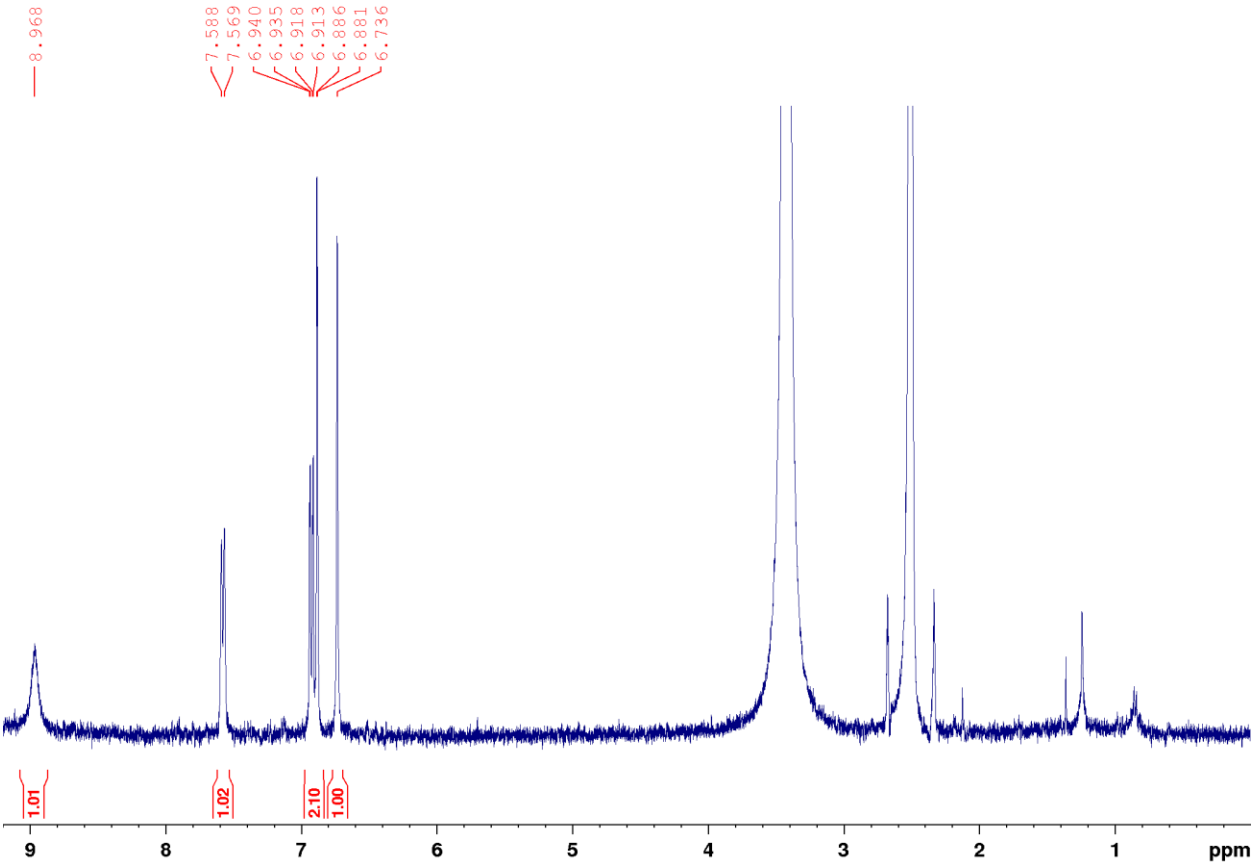

COSY NMR Spectrum of 7-hydrazineyl-4-(trifluoromethyl)-2*H*-chromen-2-one (TFCH)

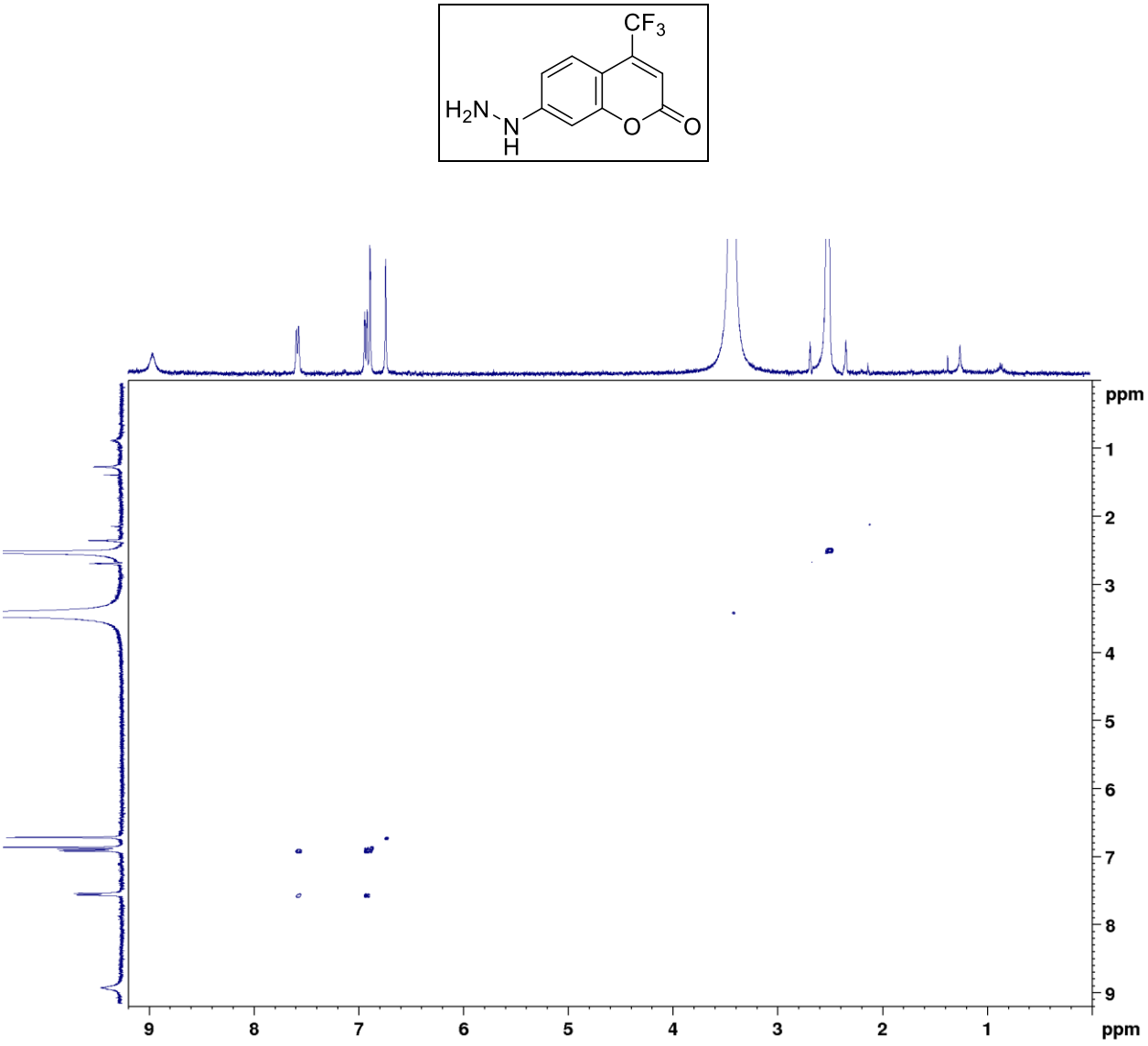

1H NMR Spectrum of ethyl 7-((ethoxycarbonyl)amino)-2-oxo-2*H*-chromene-4-carboxylate

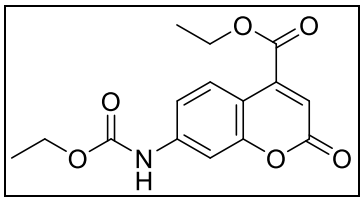

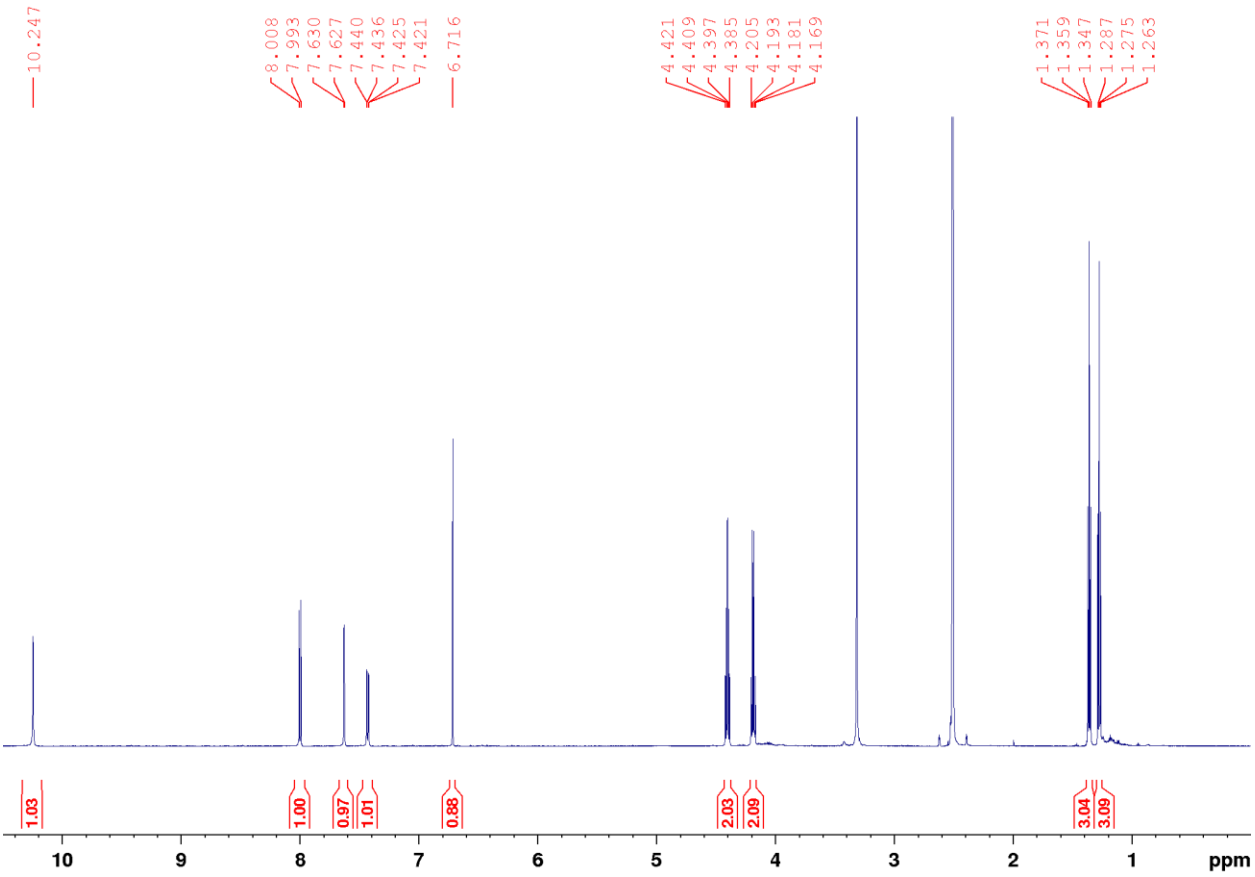

COSY NMR Spectrum of ethyl 7-((ethoxycarbonyl)amino)-2-oxo-2*H*-chromene-4-carboxylate

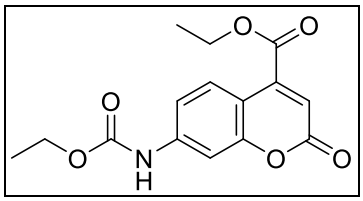

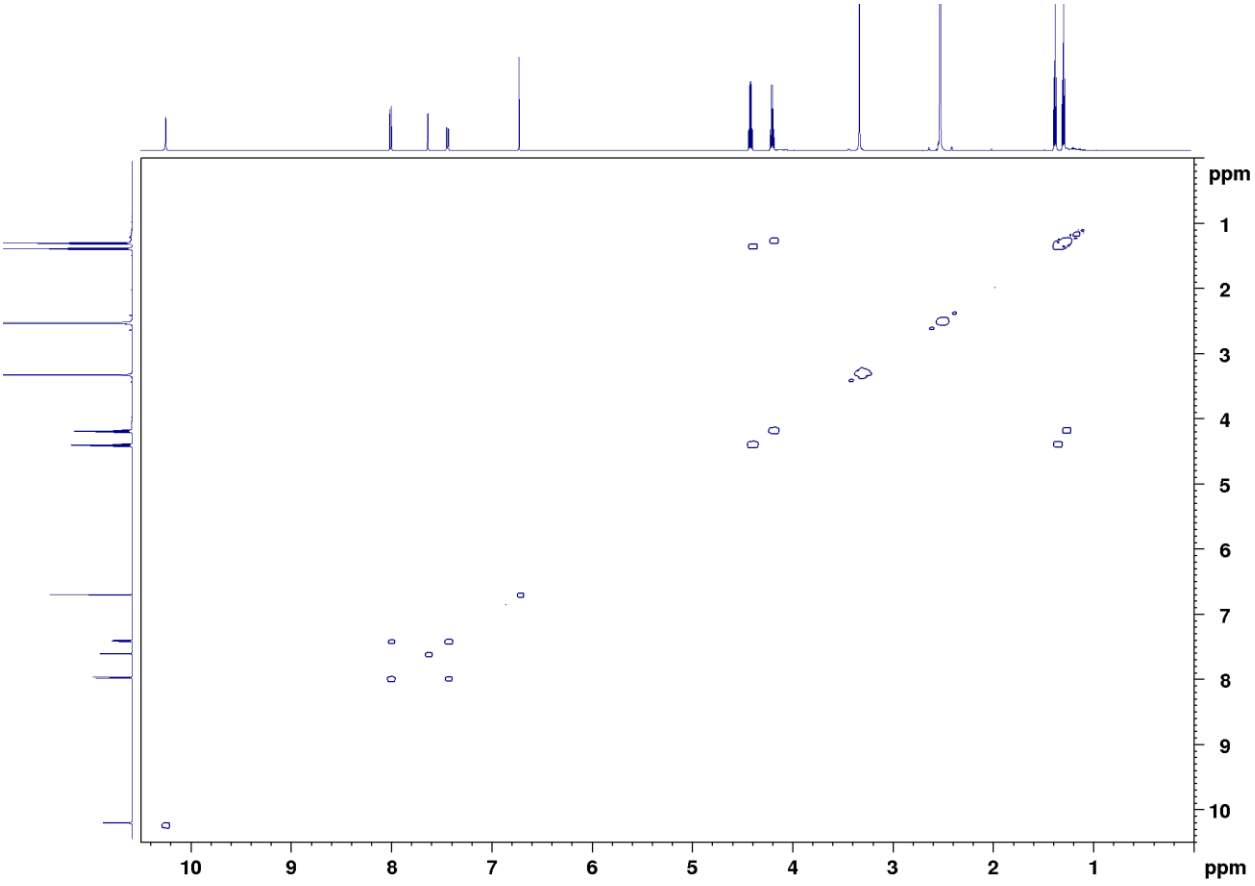

13C NMR Spectrum of ethyl 7-((ethoxycarbonyl)amino)-2-oxo-2*H*-chromene-4-carboxylate

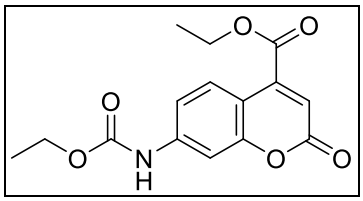

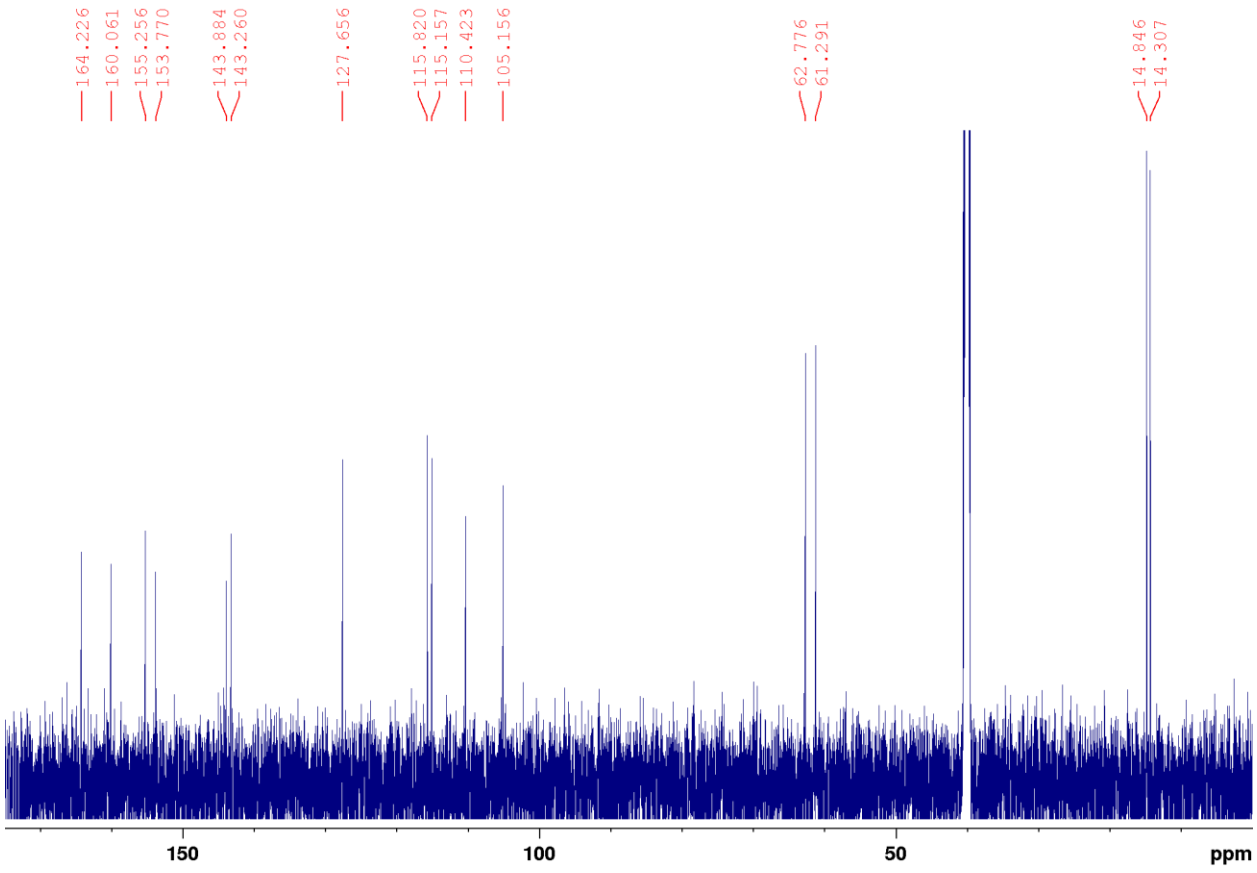

HSQC Spectrum of ethyl 7-((ethoxycarbonyl)amino)-2-oxo-2*H*-chromene-4-carboxylate

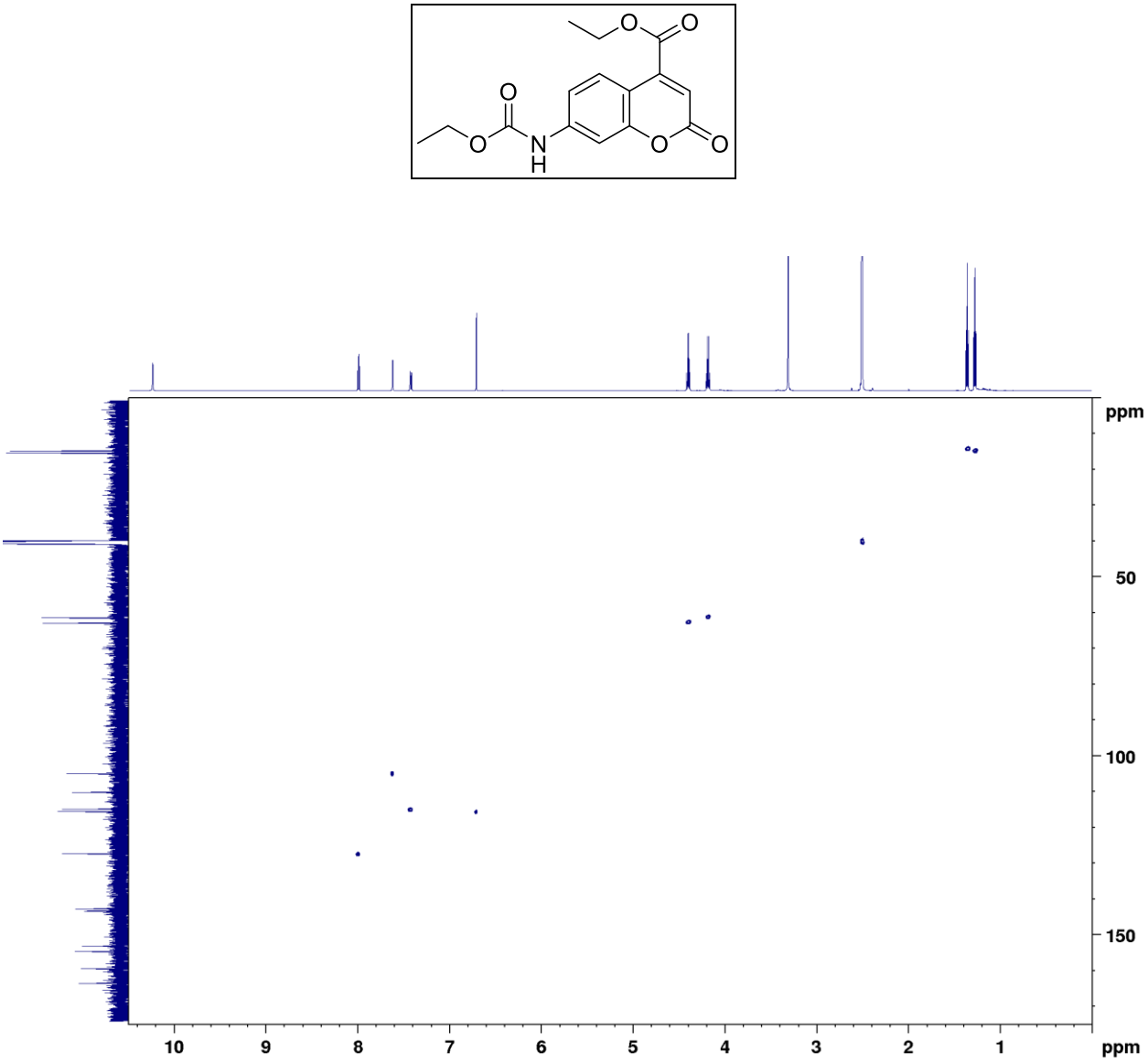

LC-MS of ethyl 7-((ethoxycarbonyl)amino)-2-oxo-2*H*-chromene-4-carboxylate

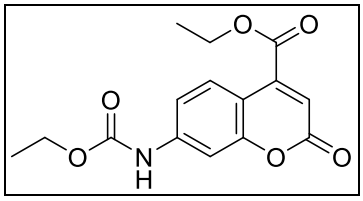

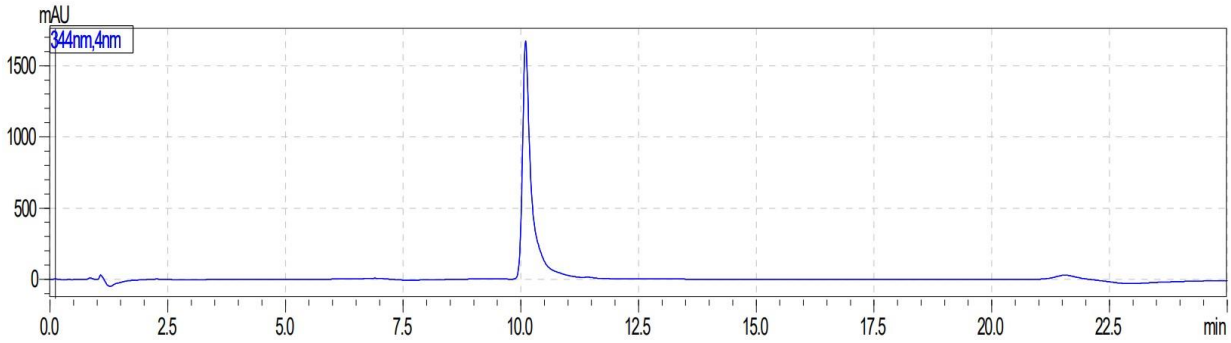

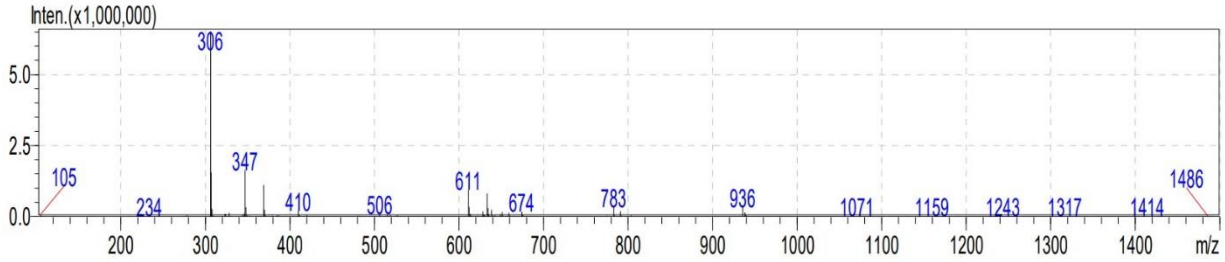

1H NMR Spectrum of 7-amino-2-oxo-2*H*-chromene-4-carboxylic acid

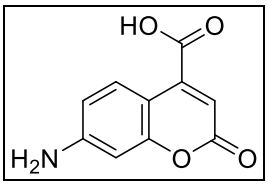

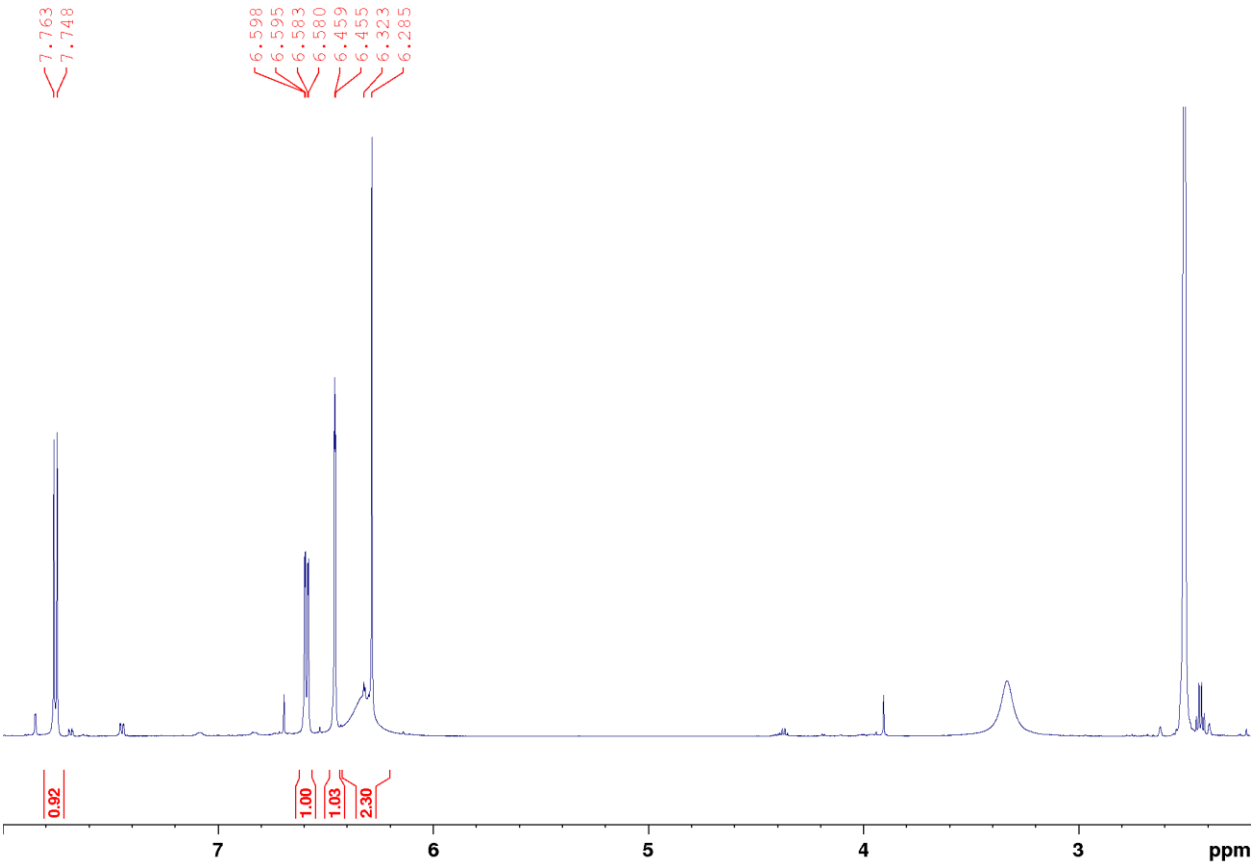

COSY NMR Spectrum of 7-amino-2-oxo-2*H*-chromene-4-carboxylic acid

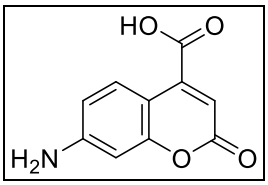

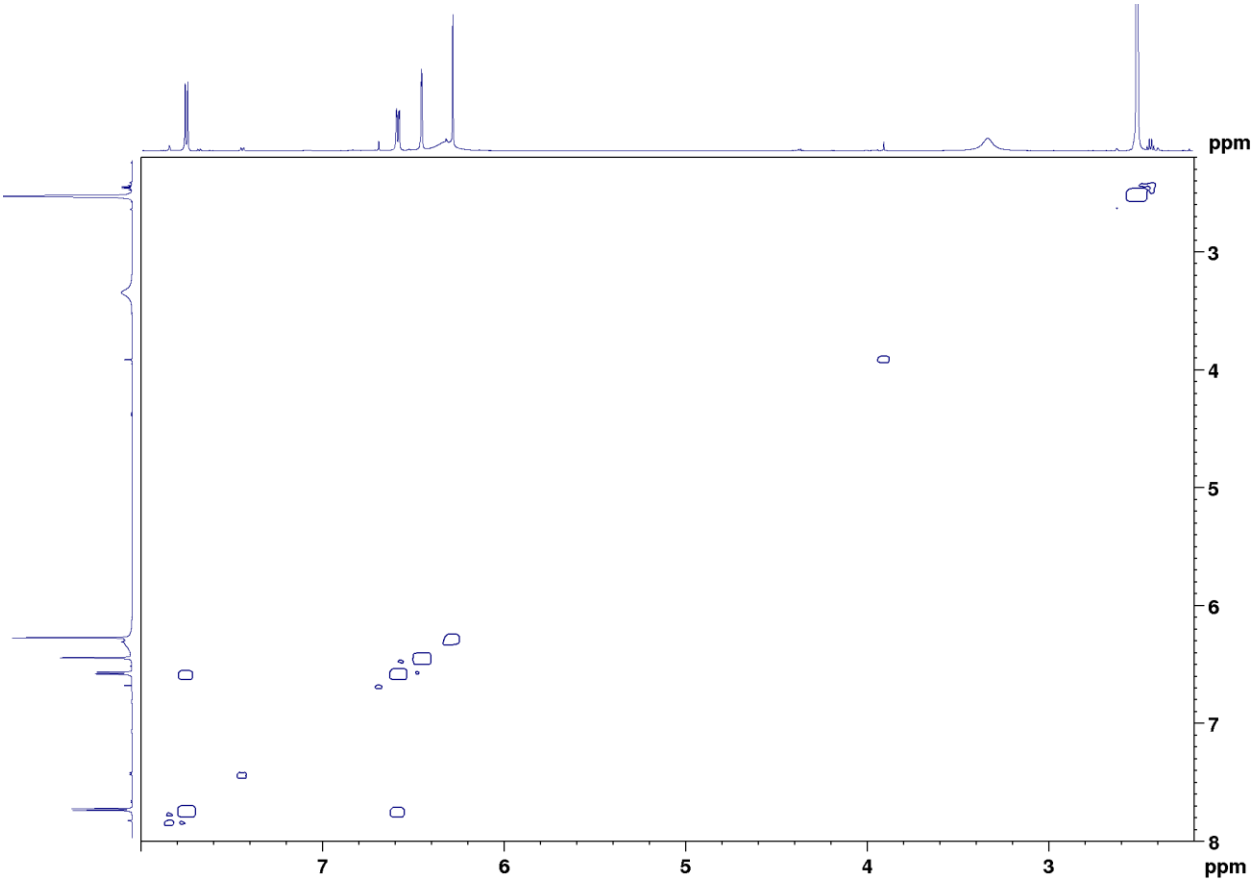

13C NMR Spectrum of 7-amino-2-oxo-2*H*-chromene-4-carboxylic acid

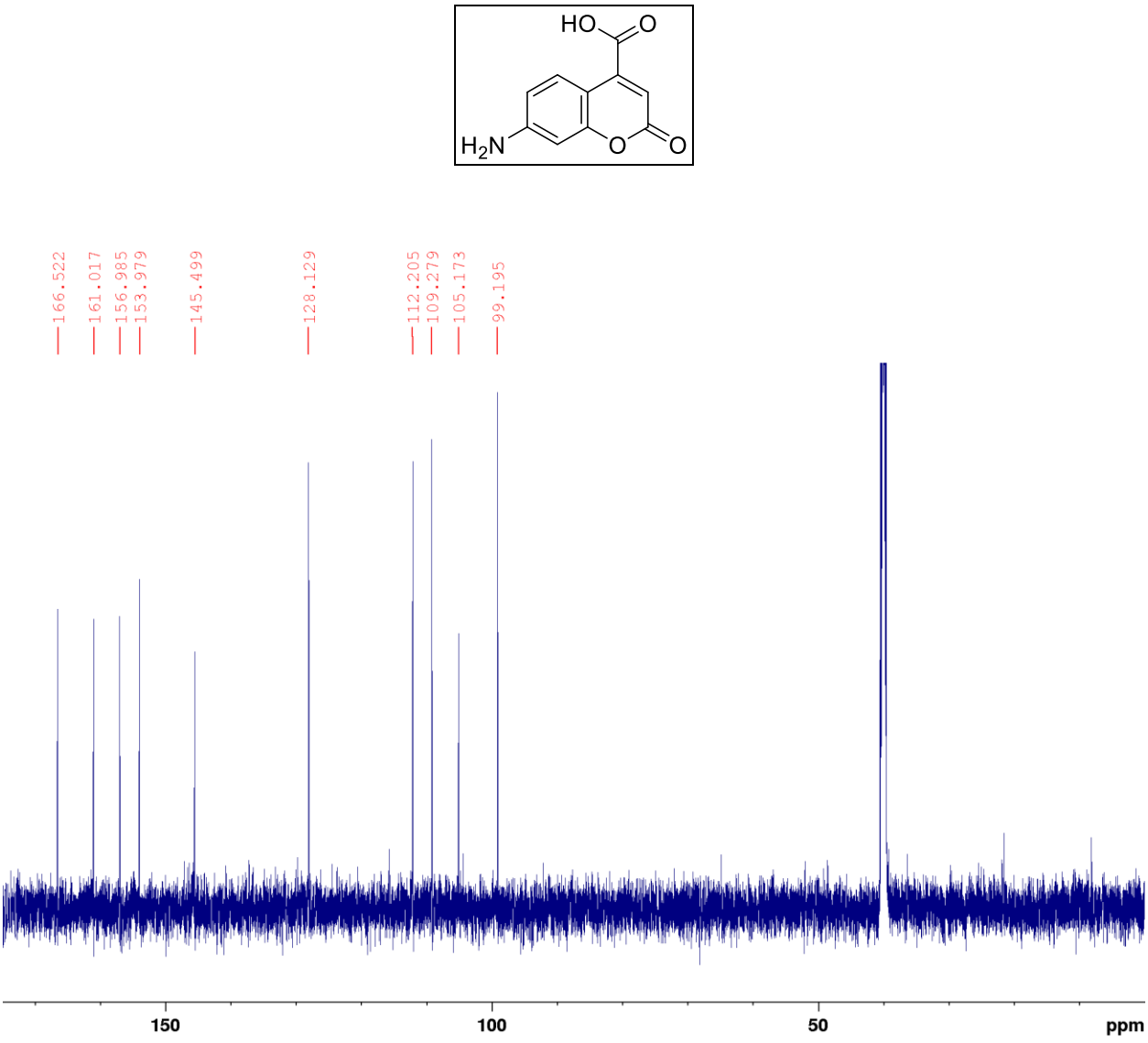

HSQC NMR Spectrum of 7-amino-2-oxo-2*H*-chromene-4-carboxylic acid

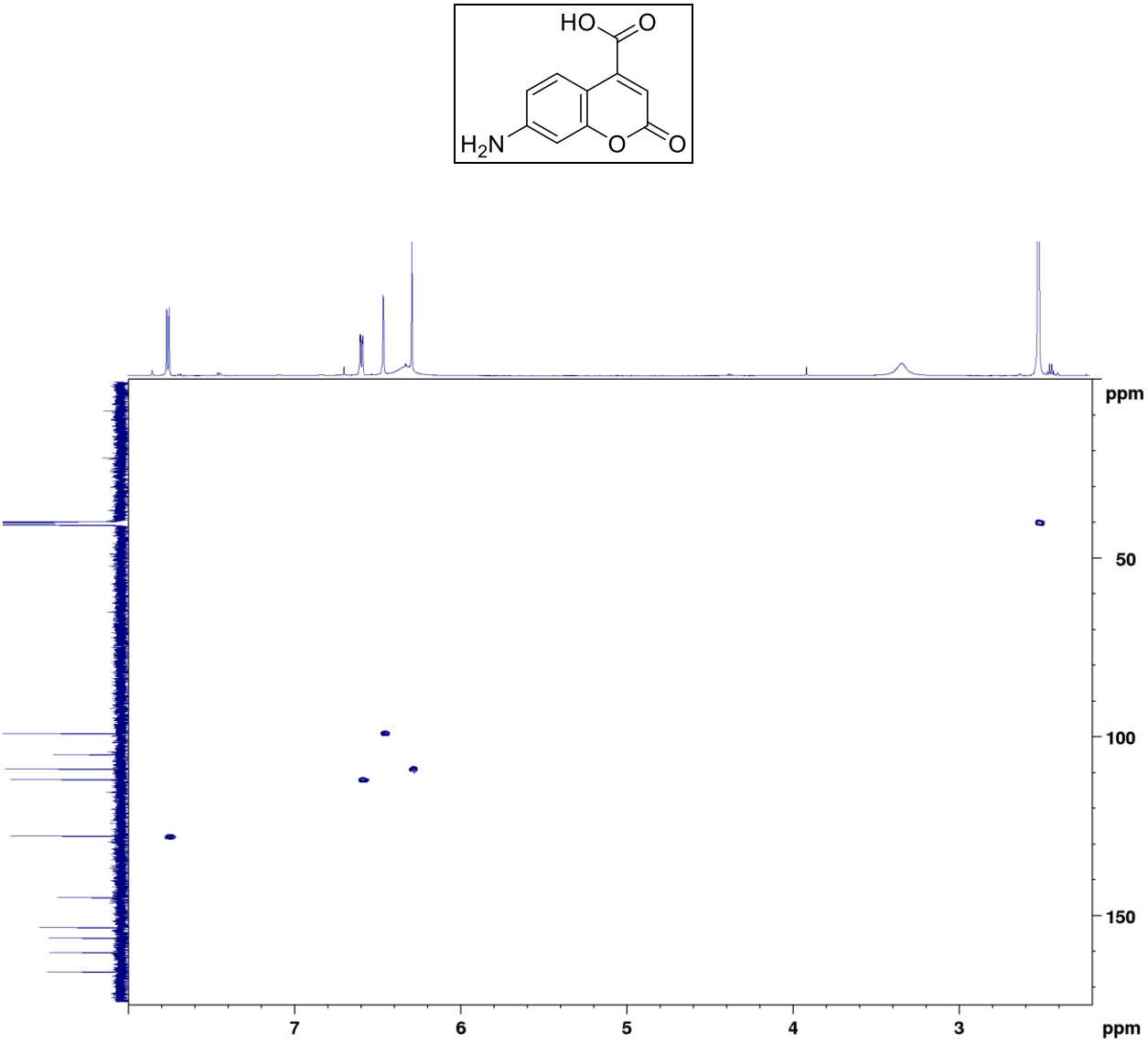

LC-MS of 7-amino-2-oxo-2*H*-chromene-4-carboxylic acid

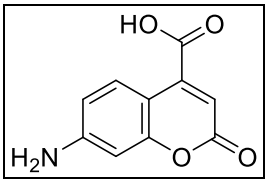

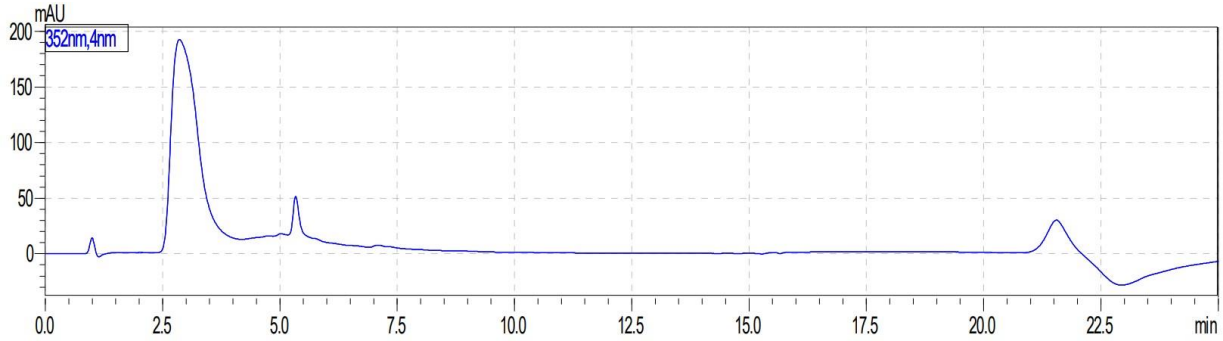

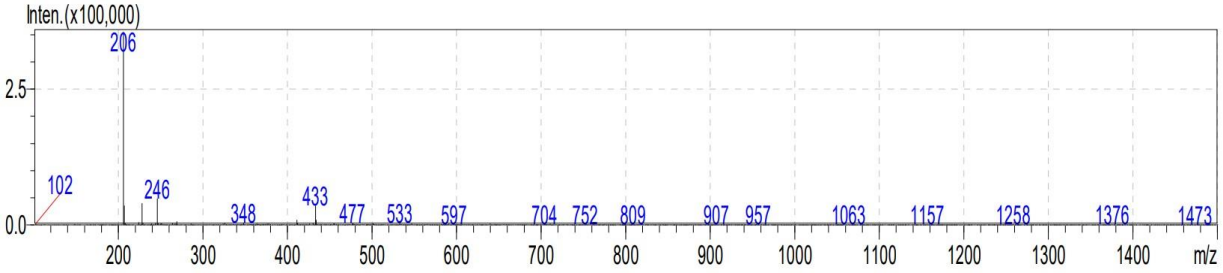

1H NMR of 7-hydrazineyl-2-oxo-2*H*-chromene-4-carboxylic acid (CAH)